MASTER THESIS

Combine remote sensing time series with community-based activity data for detecting forest change

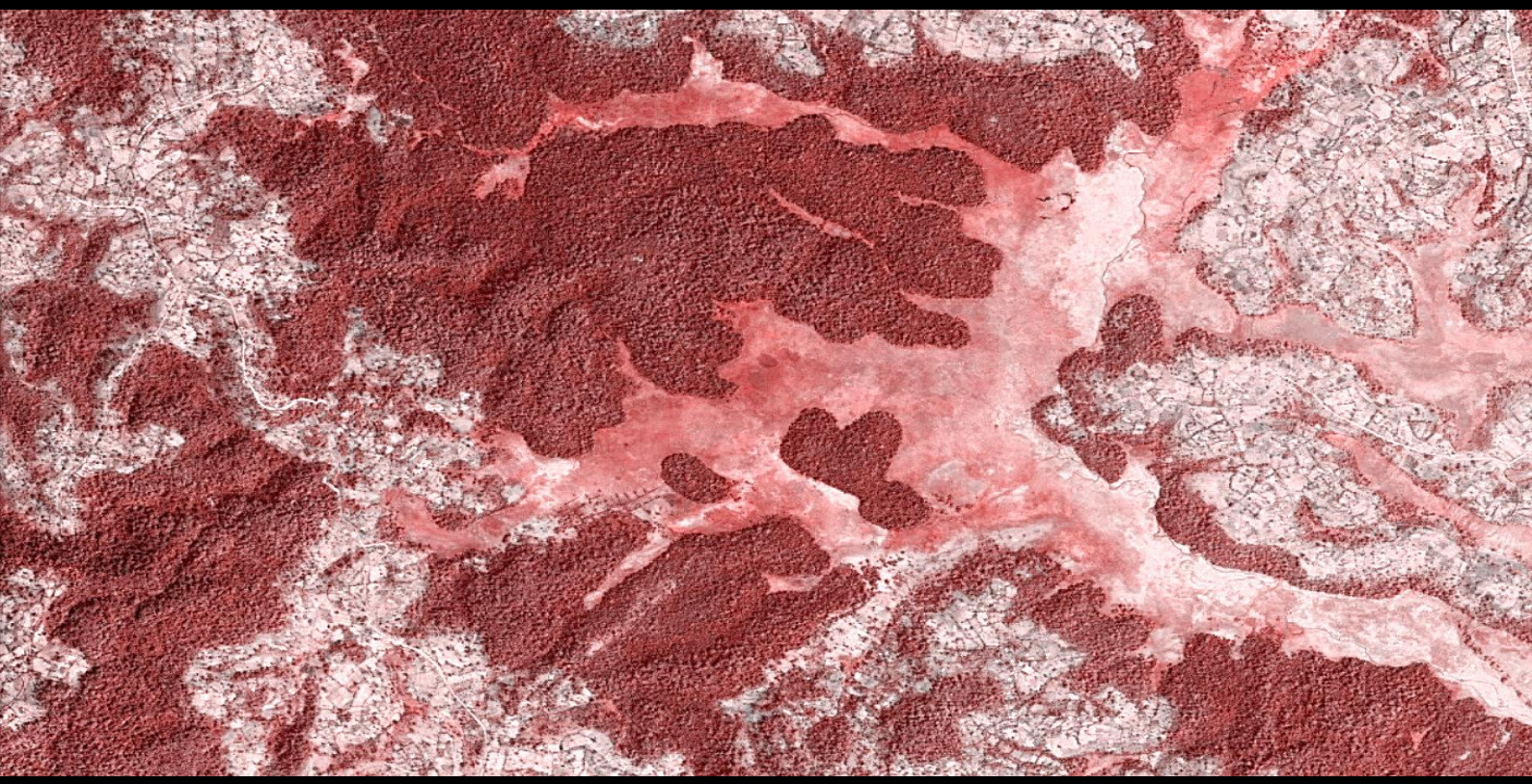

Christos Sotiropoulos

Wageningen University & Research
June 2018

Master Thesis

Combine remote sensing time series with community-based activity data for detecting forest change

Christos Sotiropoulos
Reg. No.: 800110786020

Supervisors:
Johannes Reiche
Arun Kumar Pratihast
Jan Verbesselt

Course: GRS-80436
Thesis Number: GIRS-2018-32
MSc Thesis Geo-information Science and Remote Sensing

14 June, 2018
Wageningen University
Wageningen, NL

Acknowledgments

I would like to thank my thesis supervisor Johannes Reiche for his active guidance, support and motivation throughout the process of researching and writing this thesis. I would also like to give my special thanks to Arun Kumar Pratihast and Jan Verbesselt for their support during the methodology process of this project and for exchanging ideas and opinions.

My special thanks to Jan Pokorn, who was my partner in this thesis; our different way of thinking and working made this process much more interesting.

Finally, I must express my gratitude to my family for their active support throughout my years of study. Finally, Elli for her continuous encouragement through the process of writing and finalizing this thesis.

Christos Sotiropoulos,

June 2018

Abstract

The objective of the thesis is to develop an approach to combine community-based monitoring (CBM) data with SAR (Synthetic Aperture Radar) and optical time series data streams for near real-time deforestation detection in Kafa, Ethiopia. Combining CBM and SAR-optical data promises to overcome the current limitations of optical-only forest monitoring systems that show limited temporal detection accuracies in tropical regions affected by persistent cloud cover. The integration-method builds upon an existing probabilistic (Bayesian) approach that was initially designed to combine optical and SAR time series (Reiche, de Bruin, Hoekman, Verbesselt, & Herold, 2015). Incorporation of CBM observations to this approach is the main core of the thesis. The proposed method consists of three parts; first we assess the capabilities of optical (Landsat NDVI) and SAR (ALOS PALSAR L-band, Sentinel-1 C-band) to separate forest and non-forest in Kafa. Then, the method is tested in a single pixel to evaluate the integration of the data streams, before applied in a larger area. Finally, we assess the spatial and temporal deforestation detection accuracies using reference data for the method development area. Application of the Bayesian approach in a single pixel showed that CBM observations improved the detection of deforestation 5 days earlier than with optical data streams. However, the overall contribution of CBM observations over the area was minimum (+0.35% overall accuracy, -0.12 days temporal accuracy) compared to optical data streams; as a result of their low temporal density and mostly delayed recording. Overall, CBM observations showed high potential for contribution on early deforestation detection, if only, CBM recordings are frequent.

Keywords

Community-based monitoring; remote sensing; near real-time; deforestation; Bayesian approach; Landsat; ALOS PALSAR; Sentinel-1; Kafa; Ethiopia

Table of Contents

Abbreviations

ALOS	Advanced Land Observing Satellite
BFAST	Breaks For Additive Season and Trend
BFM	BFAST Monitor
CBM	Community Based Monitoring
DP	Deforestation Probability
F	Forest
FBD	Fine Beam Double
GPS	Global Positioning System
HH	Horizontal transmit and Horizontal receive
HV	Horizontal transmit and Vertical receive
IDW	Inverse-Distance Weighting
JM	Jeffries – Matusita distance
MRV	Measuring, Reporting and Verifying
MTLc	Mean Time Lag of confirmed deforestation events
MTLf	Mean Time Lag of flagged deforestation events
NDVI	Normalized Difference Vegetation Index
NF	Non-Forest
NFMS	National Forest Monitoring System
NRT	Near Real-Time
OA	Overall Accuracy
P	Probability
PA	Producer's Accuracy
PALSAR	Phased Array type L-band Synthetic Aperture Radar
Pdf	Probability density function
PNF	Probability of Non-Forest
REDD+	Reducing Emissions from Deforestation and Degradation
RS	Remote Sensing
SAR	Synthetic Aperture Radar
SITS	Satellite Image Time Series
UA	User's Accuracy
UNESCO	The United Nations Educational, Scientific and Cultural Organisation
VH	Vertical transmit and Horizontal receive
VV	Vertical transmit and Vertical receive

1. Context and Background

Tropical forests are of fundamental importance to humanity as they provide habitats for numerous species, maintain water cycle, stabilize soil, provide wood and other goods and regulate the local and global climate (European Parliament (2016); Fagan & DeFries, 2009). Deforestation and forest degradation lead to the loss of these important ecosystem services and are regarded as one of the major sources of greenhouse gas emissions (Harris et al., 2012; Zarin, 2012). In order to reverse the increase of global carbon dioxide emissions an international initiative on Reducing Emissions from Deforestation and Degradation (REDD+) is currently activated to mobilize developing countries under a common strategy of mitigating climate change by reducing forest cover loss and forest degradation (Angelsen, 2008; Fagan & DeFries, 2009; Gullison et al., 2007).

One of the basic targets of participating countries in REDD+ program is the development of a robust and transparent national forest monitoring system (NFMS) in order to accurately, cost-effectively and consistently over time, detect forest area changes (UNFCCC, 2009). Under these conditions, the combination of remote sensing (RS) and ground based data are officially suggested by REDD+ as essential data sources for Measuring, Reporting and Verifying (MRV) (UNFCCC, 2009) the four main monitoring objectives of change; location, area, time and driver of forest change (Pratihast et al., 2014). Moreover, timely information on deforestation, particularly illegal loggings, is essential in order to improve the management and protection of tropical forest resources by mobilizing governmental authorities and local communities and enacting immediate law enforcement (Assunção, Gandour, & Rocha, 2014; Lynch, Maslin, Balzter, & Sweeting, 2013; Wheeler, Hammer, Kraft, & Steele, 2014).

Satellite Image Time Series (SITS) are considered as the primary data source for forest change detection in near real-time (NRT) (Lynch et al., 2013). SITS can provide a collection of satellite images over vast forest areas (Lynch et al., 2013), taken from the same location at different dates. The repetitive observations of these data streams is unique and allow the detection of forest cover changes over time where vegetation appear more easily discriminable than by analysing single images (Guyet & Nicolas, 2016; Hansen et al., 2013; Lynch et al., 2013). In this context, NRT forest monitoring is based on the analysis of every image on the time series, as soon it is acquired, with the advantage of having dense information of rapid updates and historical dynamic of the target.

Last years, due to open data policies, medium resolution remote sensing imagery has become freely available and has extensively used to detect small-scale forest cover changes, while offering regional to global scale products (De Sy et al., 2012; Hansen & Loveland, 2012; Hansen et al., 2013; Lu, Li, & Moran, 2014). This sparked considerable development in optical time series based monitoring methods, increasing their use over conventional bi-temporal approaches for forest change detection (Banskota et al., 2014). Optical time series methods provide an improved NRT forest change monitoring over large areas with high temporal resolution and accuracy (DeVries, Verbesselt, Kooistra, & Herold, 2015; Dutrieux, Verbesselt, Kooistra, & Herold, 2015; Reiche et al., 2015; Zhu, Woodcock, & Olofsson, 2012). As a result, they allow rapid detection of forest disturbance while offering better descriptions of forest change trajectories than with traditional methods (Huang et al., 2010; Kennedy, Yang, & Cohen, 2010). However, persistent cloud cover in tropical regions reduces the availability of clear observations from optical sensors (Lehmann et al., 2012; Verbesselt, Zeileis, & Herold, 2012; Walker, Stickler, Kellndorfer, Kirsch, & Nepstad, 2010). This is a common phenomenon in the tropics with some countries experiencing annual

average cloud cover rates of more than 80% (Herold, 2009). As a result, clouds limit the optical coverage from remote sensors and often prevent rapid change detection of deforestation and forest degradation.

Synthetic Aperture Radar (SAR) penetrates through clouds and smoke haze, and can acquire data day or night under all weather conditions (Achard et al., 2010; Shimada, 2010). This gives a considerable advantage over optical satellite data when monitoring tropical forests. SAR systems can operate at different wavelengths. Due to its longer wavelength (~25cm), L-band SAR penetrate the forest canopy and scattering occurred by the ground, branches and trunks results in higher backscatter than non-forest areas like bare land and water. In addition, L-Band SAR cross polarisation (HV) has demonstrated to improve further the discrimination between forest and non-forest areas than co-polarisation (Rahman & Sumantyo, 2010) while HVHH backscatter ratio has shown to be more sensitive to deforestation than HH or HV (Reiche, 2015). L-band SAR time series data by ALOS (*Advanced Land Observing Satellite*) PALSAR (*Phased Array type L-band Synthetic Aperture Radar*) has been successfully used for mapping and monitoring forest change; particularly in tropical regions (Almeida-Filho, Shimabukuro, Rosenqvist, & Sanchez, 2009; Motohka, Shimada, Uryu, & Setiabudi, 2014; Rahman & Tetuko Sri Sumantyo, 2012; Ryan et al., 2012; Shimada et al., 2014; Whittle, Quegan, Uryu, Stüewe, & Yulianto, 2012). On the other hand, C-band SAR operates at shorter wavelength (~6cm) interacting mainly with the top layer of the forest canopy; leaves and twigs. Reiche (2015) mentions that this returns a lower backscatter contrast between forest/non-forest areas than L-band SAR indicating C-band lower sensitivity to forest cover changes. Nevertheless, C-band has also been used for mapping and monitoring forest change while the combination of C and L band has shown to increase the distinction between woodland and forest areas (Haarpaintner, Davids, Hindberg, Zahabu, & Malimbwi, 2015), and is likely to better identify forest degradation. On 2014, Sentinel-1 satellite was launched, providing for the first time, dense C-band SAR time-series data over tropical forest areas free and openly (Reiche et al., 2016). The significant potential of Sentinel-1 for monitoring forest changes however, still needs to be explored (Reiche et al., 2016). At the downsides of SAR systems are the false detections mainly occurred by forest degradation activities (Ryan et al., 2012); such in cases after clear-forest-cuts where trunks are left on the ground for a long period and result in higher backscatter signal (Kellndorfer, Cartus, Bishop, Walker, & Holecz, 2014), and the low density of L-band SAR observations per year in tropical countries (Rosenqvist, Shimada, Ito, & Watanabe, 2007).

Deforestation monitoring in NRT using a single optical or SAR data stream is limited by the relatively low density of valid observations per year that leads to late detection of changes. Therefore, integrating SAR and optical data can increase the temporal accuracy and as a result decrease the delay of change detection (Hussain, Chen, Cheng, Wei, & Stanley, 2013; Lehmann et al., 2012; Reiche, 2015; Zhang, 2010). Fusion of optical and radar imagery has successfully demonstrated to increase forest mapping and deforestation detection accuracy (Erasmi & Twele, 2009; Kuplich, 2006; Laurin et al., 2013; Walker et al., 2010). However, integration of SAR-optical time series is limited to date and rather ambiguous as various challenges have to be addressed including; co-registration accuracy and image acquisition at different dates (Reiche, 2015). Lehmann et al. (2015) used the Bayesian classification framework (Strahler, 1980) and successfully applied a multi-temporal approach to integrate Landsat and ALOS PALSAR annual data streams for forest change detection (Reiche, 2015). Moreover, Reiche (2015), by using a probabilistic approach based on Bayesian framework managed to effectively integrate medium

resolution ALOS PALSAR and Landsat NDVI time series for NRT deforestation detection. This approach was based on calculating forest probabilities from each newly acquired image at SAR and optical data streams to quickly identify deforestation events (Reiche, 2015). Results of Bayesian change detection approach have demonstrated higher spatial and temporal accuracies than with single sensors approaches (Reiche, 2015).

In the last few years, community based monitoring (CBM) from local citizens and experts have gained much attention as a way to increase local participation and ensure the sustainability of REDD+ forest monitoring programmes (Boissière, Beaudoin, Hofstee, & Rafanoharana, 2014; Conrad & Hilchey, 2011). Due to its low cost (Pratihast et al., 2012), CBM can be promising in applications such as forest carbon estimation and forest change monitoring (Brofeldt et al., 2014; Pratihast et al., 2014). Communities local knowledge can greatly enhance the recording of forest change activities (deforestation, forest degradation or reforestation) and provide important information regarding the location, time, size and driver of forest change on a NRT basis (Pratihast et al., 2014; Skutsch, Torres, Mwampamba, Ghilardi, & Herold, 2011). Such information is rarely captured comprehensively from remote sensing systems, thus, local participation within forest monitoring programs has the potential to advance the REDD+ MRV implementation (Pratihast et al., 2014). The recent development of mobile phone technologies has improved the quality of data collection procedures and thus, can enhance continuous data acquisition, "transforming" local communities to active ground based sensors (Goodchild, 2007; Pratihast et al., 2012). However, since data collection is performed independently from local participants' inconsistencies, limitations and reliability issues regarding their accuracy has often been addressed (Danielsen, Burgess, Jensen, & Pirhofer-Walzl, 2010; Fry, 2011; Pratihast et al., 2014). These issues include; inconsistencies in monitoring frequency due to weather conditions, limited spatial coverage due to inaccessible locations, and unreliable data collection procedures (Pratihast et al., 2014). Proper recruitment and training of local experts can reduce the effect of these obstacles and thus, allow the integration of CBM data streams in NFMS (Conrad & Hilchey, 2011; Skarlatidou, Haklay, & Cheng, 2011). To this date, CBM data has mostly used as reference data for training and validating time series based methods for forest monitoring.

2. Problem Definition

Local participation within REDD+ forest monitoring programs can ensure their sustainability and has the potential to advance the MRV implementation (Pratihast et al., 2014). Pratihast et al. (2014) showed that CBM data collected by local forest experts in southern Ethiopia had accurately provided the spatial and temporal details of forest change and in many cases enhanced remote sensing-based results for forest cover change. Therefore, integration of CBM observations in NFMS may improve NRT forest monitoring as they can provide additional understory description of deforestation, increase the number of observations, and improve the spatio-temporal and thematic quality of deforestation estimates. However, combining CBM observations with SAR-optical SITS holds no prior knowledge and further research on developing a functional approach is needed.

Prior to data-integration approach, evaluating the F/NF separability of optical and SAR SITS is essential. Separability of F/NF classes distribution is related to SITS sensitivity on deforestation detection. This allows the identification of the sensor metric with the higher sensitivity capability to detect deforestation. It is also important in the case of C-band SAR which is known to have less

sensitivity to forest cover changes compared to L-band (Mitchell et al., 2014). As a result, F and NF distributions of C-band SAR data-stream are expected to overlap more demonstrating a lesser performance on distinguishing the two classes (Reiche, 2015). This may lower the deforestation detection performance of the proposed integration approach. Therefore, F/NF separability of C-band SAR is of particular interest in order to assess its usefulness to the selected integration approach. Currently, there is little knowledge on the capabilities of C-band Sentinel-1 for forest change monitoring (Reiche, 2015).

Integration of CBM-SITS is the main core of the thesis and lies upon the development of a functional approach to fuse local observations with time series data. Latest developments on SITS data-integration approaches have indicated the high potential of the probabilistic Bayesian change-detection method. This probability-based approach has been successfully used in Reiche (2015) study to combine medium resolution SAR and optical time-series and shows potential of further development in order to embed additional data streams. The Bayesian approach is primary based on deriving and combining F/NF probabilities of each observation at SAR-optical SITS (Reiche, 2015). This means that embedment of CBM data into the Bayesian probabilistic framework requires similarly the prior conversion of each CBM observation into conditional F/NF probabilities. However, each CBM observation consists of a series of attributes regarding the location, area and intensity of forest disturbance (among others). Therefore, proper analysis and interpretation of these attributes in order to derive realistic F/NF probabilities is crucial part of the method.

Post-integration results are important to be evaluated; particularly CBM contribution for NRT deforestation detection. Therefore, an assessment of spatial and temporal accuracy between CBM-SITS and SITS integration-approach is essential.

3. Research Objective and Research Questions

The objective of the thesis is to develop an approach to combine CBM and SITS data streams for NRT deforestation detection. The following key research questions arise:

1. What are the capabilities of optical (Landsat NDVI) and SAR (ALOS PALSAR L-band, Sentinel-1 C-band) to separate forest and non-forest in Kafa Biosphere Reserve?
2. How can CBM observations and SITS be combined in a probabilistic framework for NRT deforestation detection?
3. How does the spatial and temporal accuracy of deforestation detection improves by combining CBM observations and SITS?

4. Feasibility and Risks

All software packages required for this study are freely available from Wageningen University. In addition, both CBM and SITS data provided pre-processed and co-registered, and ready for analysis.

Aim of this thesis is the development of a novel approach for NRT data-stream based forest monitoring. The basic core of the approach has been applied successfully in recent study (Reiche, 2015); however, the need of integrating additional data sources requires further development of

the method and can be challenging. In order to reduce the uncertainty and avoid unknown factors, a set of simplifying assumptions is created:

- The only type of forest change covered is deforestation. Forest degradation is not covered.
- Areas of steep slopes are not covered as terrain variations can affect radar geometry.
- Low quality community based data are rejected.
- Seasonality will be ignored.

5. Data & Methods

5.1. Study Area and Data

The study area is located in the UNESCO Kafa Biosphere Reserve in south-western Ethiopia. It is an area over 700,000 ha in size with a variation in altitude ranging from 1400 to 3100 m (Pratihast et al., 2016). Kafa is characterized by Afromontane cloud forest vegetation, with forests covering approximately half of the land (Schmitt, Denich, Demissew, Friis, & Boehmer, 2010). The forest ecosystem consists mostly of highly fragmented moist evergreen forests, forest-cropland matrix landscapes and coffee trees (DeVries et al., 2013). Smallholder agriculture and industrial coffee and tea plantations are considered as the main drivers of deforestation and forest degradation in the reserve (Schmitt, Senbeta, Denich, Preisinger, & Boehmer, 2010).

The area for method development is located approximately at the north-center of the Kafa Biosphere Reserve (fig. 1). It is selected because of its flat terrain and clear signs of forest disturbance. The main driver of deforestation and forest degradation is agricultural expansion.

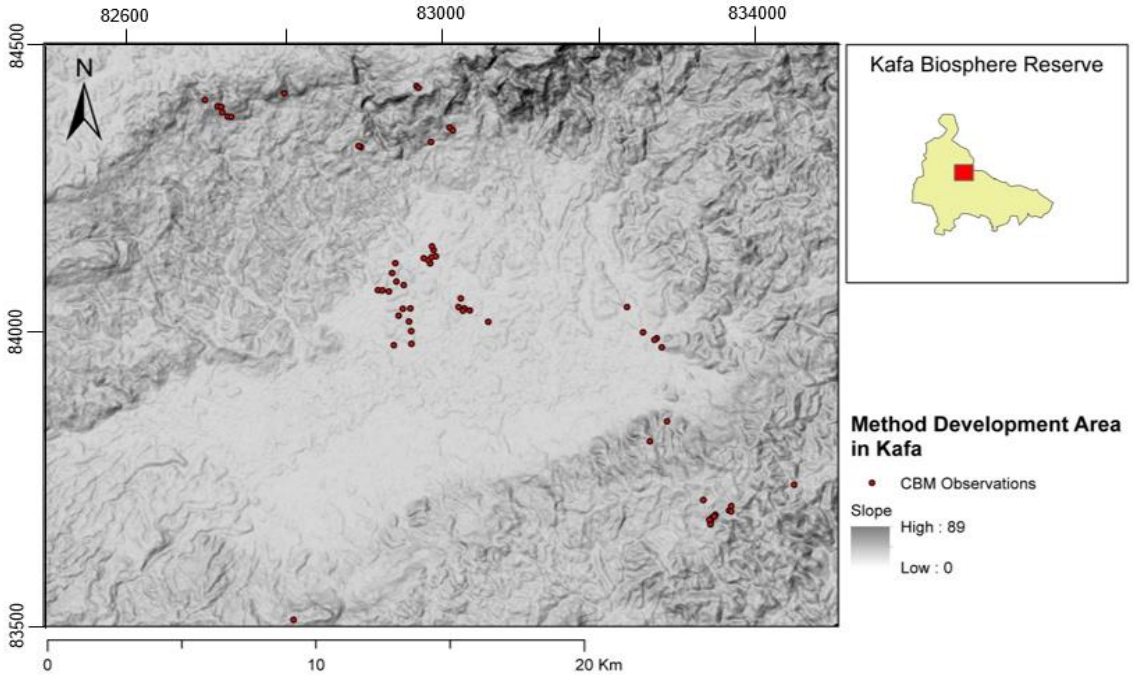

Figure 1: Area for method development

CBM data were collected by 30 forest rangers who were recruited to implement forest management and monitoring activities within the Kafa reserve (Pratihast et al., 2014). Forest rangers were trained primarily in methods and tools to record disturbances (deforestation and

degradation) and positive forest changes (afforestation and reforestation), in a consistent manner (DeVries, Pratihast, Verbesselt, Kooistra, & Herold, 2016). Recording tools included disturbance forms, Global Positioning System (GPS) devices, and mobile devices with integrated GPS and camera functionality (Pratihast et al., 2014). Each CBM observation contain description in a range of attributes regarding forest status and history and is linked with a plot description, coordinates and five photos (facing north, east, south, west and upwards) (DeVries et al., 2016). Details of these reports have also been described in detail in Pratihast et al. (2014). For this study low quality CBM data have been rejected. In the end, a total of 17 CBM observations were proper to be used. All CBM observations were acquired in Kafa Biosphere Reserve during March, 2015.

The SITS data comprises three time-series stacks (i) Landsat NDVI for the years 2010 to 2016, (ii) ALOS PALSAR FBD (Fine Beam Double) Polarisation HH/HV for the years 2007 to 2016 and (iii) Sentinel-1 VV for the years 2015 to 2016. All RS data streams provided pre-processed and co-registered by Johannes Reiche. The number of valid SITS observations for the method development area during 2015-2016 is depicted in figure 2.

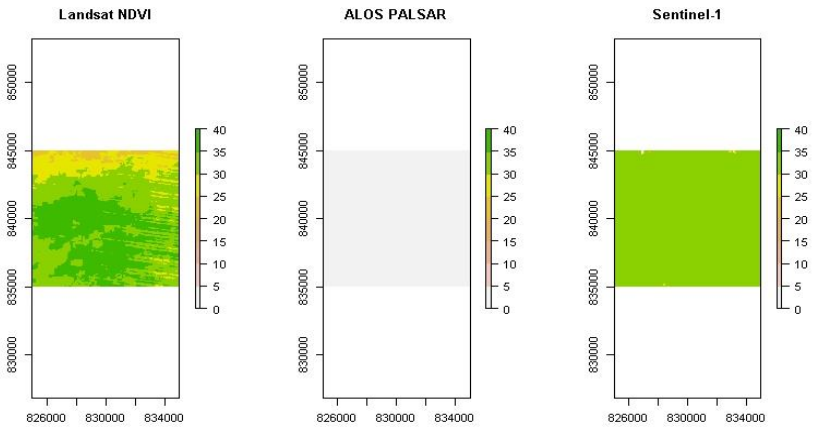

Figure 2: Number of valid SITS observations for the method development area during 2015-2016

5.2. Methods

The research comprises the (i) F/NF separability analysis of SITS (research question 1), (ii) pixel and field based development of a CBM-SITS integration method for NRT deforestation detection (research question 2) and (iii) data-integration method validation. The validation assesses the spatial and temporal accuracy between CBM-SITS and SITS integration-approach in order to evaluate the CBM contribution (research question 3). See Figure 3 for a schematic illustration.

All developing steps were conducted in R (R Development Core Team, 2013), supported by ArcGIS and Google Earth for visualisation.

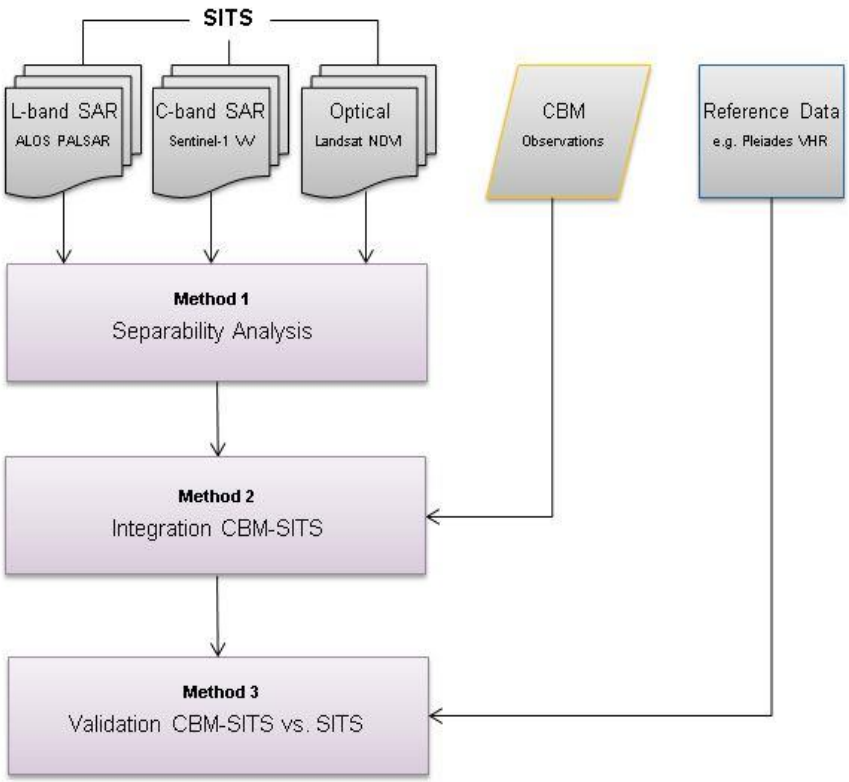

Figure 3: Schematic representation of research method. The steps are described below in more detail.

5.2.1. Forest/Non Forest Separability analysis

This method assesses the capabilities of SITS (Landsat NDVI, ALOS PALSAR L-band, Sentinel-1 C-band) to separate forest and non-forest in Kafa Biosphere Reserve. Method applied both for original and deseasonalised time series data and consists of a signature and separability analysis.

SITS have been deseasonalised using spatial context. Spatial context approach involves the spatial normalization of each pixel in the time series using the median value of adjacent pixels whose values exceed the 90th percentile (Hamunyela, Verbesselt, & Herold, 2016).

Signature Analysis

Signature analysis is centred on the generation of signatures from forest (F) and non-forest (NF) classes. In order to identify the classes, seven training samples were collected for each class by visual interpretation of the study area (fig.4). Special consideration was given on selecting samples that remain unchanged over the spatial domain of the time series data. To ensure this, a mask presenting stable forest areas was used as reference map (provided by J. Reiche). The selected forested samples consist mostly of evergreen forest formations while non-forested samples from bare soil and at a smaller percent, low vegetation (90% and 10% approx.). After selection, the training samples are merged into each class and F/NF signatures, mean and standard deviation, are collected for each SITS.

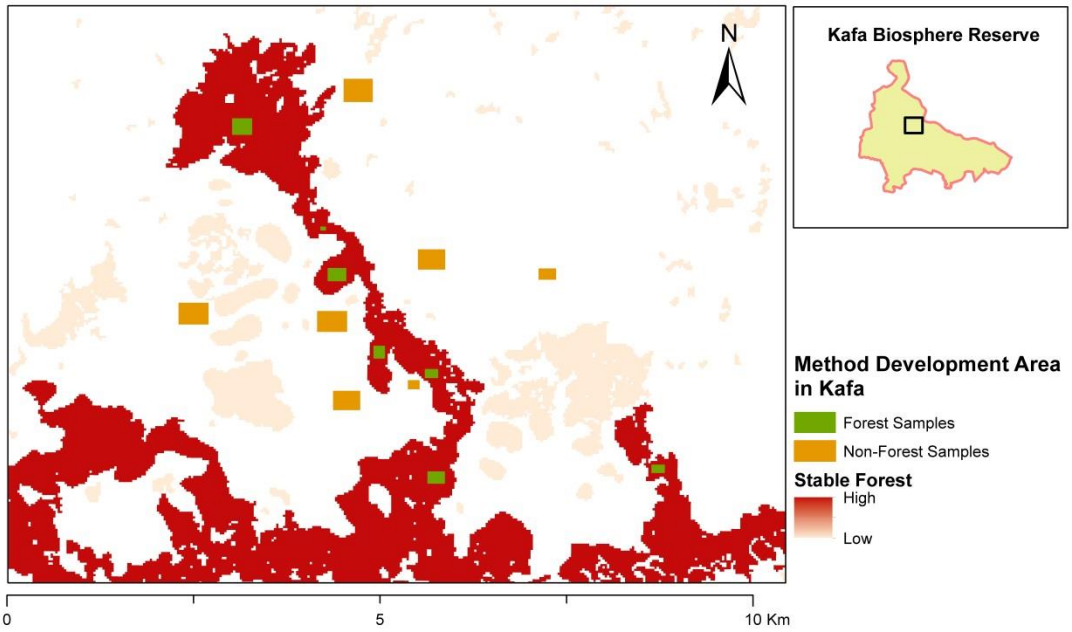

Figure 4: Selection of forest and non-forest samples in the method development area using a stable forest mask

Separability analysis

Separability analysis was based on the Jeffries – Matusita Distance (JM) between the F and NF classes and calculated separately for each data stream. JM evaluates the class overlap of F and NF distributions and measures their separability on a scale of 0 (inseparable) to 2 (separable).

5.2.2. Integration of CBM-SITS for NRT deforestation detection

For the combination of CBM observations with SITS we build upon a probabilistic Bayesian framework described in Reiche (2015) study. Method is tested in a single pixel to evaluate the integration of the data streams, before applied in a larger area. The main steps of the Bayesian approach are described here and a schematic illustration is shown in fig.5:

- Step 1 consists of the derivation and combination of F/NF conditional probabilities for each individual data steam observation (Reiche, 2015). For SITS observations, conditional probabilities derive from the corresponding sensor specific F/NF probability density functions (pdfs) (Reiche, 2015). Pdfs are identified using the F/NF training samples from separability analysis. For CBM observations, conversion into F/NF probabilities is more challenging and is described below.
- In Step 2, observations at time t with NF probability that exceeds 0.5 are flagged to be potentially deforested. Then, the deforestation probability for a flagged observation is calculated using iterative Bayesian updating which takes into account the previous (t-1), the current (t), and the upcoming observations (t+1) (Reiche, 2015). In the end, iterative Bayesian updating confirms or rejects a deforestation event at time t (Reiche, 2015).

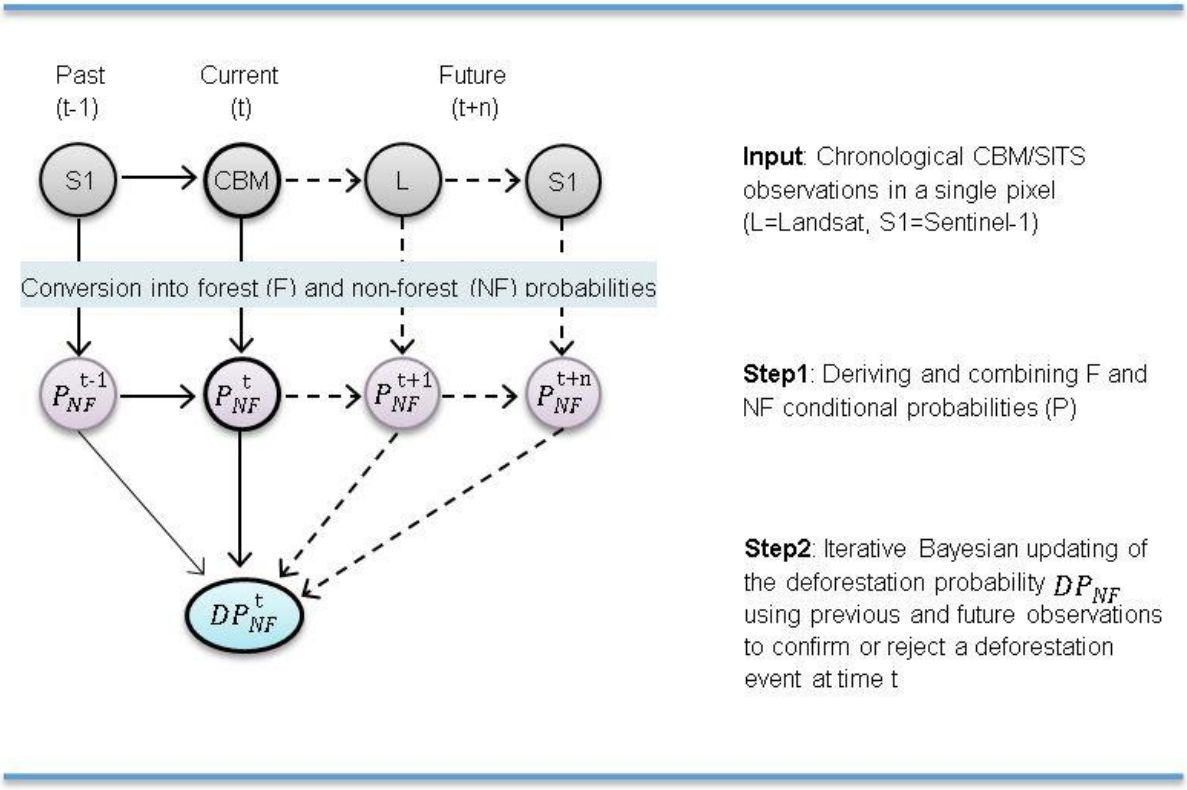

Figure 5: Schematic illustration of the proposed Bayesian approach

Derive F/NF probabilities from CBM observations

As described before, each CBM observation consists of a series of attributes such as; date, coordinates and area of change. Conversion of each observation into F/NF conditional probabilities requires proper interpretation of these attributes.

Coordinates, provided in longitude and latitude, can help us identify the location of the CBM observations. Since, every SITS has the same extent and resolution the CBM observations correspond to the same point locations for all the time series. These are the standing points at which forest rangers recorded deforestation therefore we assume that these points have the higher NF probability; 0.95 or 95%.

The area of change is provided in hectares (ha) and it is assumed to represent the area around the CBM observations. Spatial depiction of the disturbed area can be occurred by buffering the observation-points at an extent (radius) of equal size to the recorded area of change (fig. 6). This circular buffering captures all pixels which centers contact or included within the buffered area. At this point, a forest mask is used to extract the stable F part and capture the actual area of change.

Final step is to assign NF probabilities to the captured pixels. For this we have to take into account that deforestation intensity within a disturbed area is distributed differently and it is unpredictable. In order to simulate it as possible, we start from the known CBM observation point which has the higher NF probability, 0.95, and assume an inverse-distance weighting (IDW) interpolation towards the edges of the area of change. In order to apply the IDW interpolation we

use a linear function which calculates the NF probability of a pixel-center based on its distance from the CBM observation point. At maximum distance, max d, pixel get the minimum PNF value; 0.5. The function used is shown in figure 6.

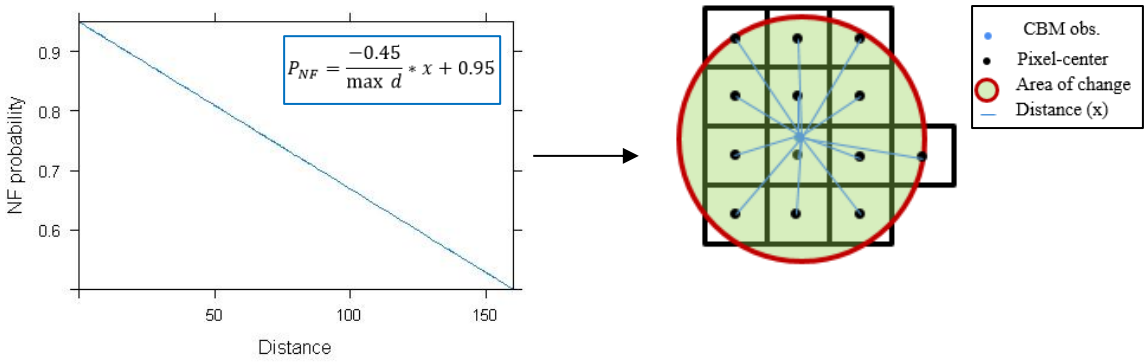

Figure 6: Schematic illustration of the IDW function used to convert CBM observations to NF probabilities. Each pixel gets the NF probability of its center and the date of the CBM recording. x = the distance between the CBM observation point and pixel-center. max d = the longest distance between two points within a disturbed area, representing the diameter of the largest recorded CBM area; 2Ha ≈ 160 meters diameter

Pixel-based approach

Based on the above mentioned, we test the main method in a single pixel to evaluate the integration of the data streams.

Pixel corresponds to a CBM observation and located within the area of change. Test pixel is located within an area of 0.5 ha, disturbed by locals for charcoal production and recorded from forest rangers on March 2015. Google Earth images available for the area are from 2014 and 2016, before and after the monitoring period; 2015 (fig. 7).

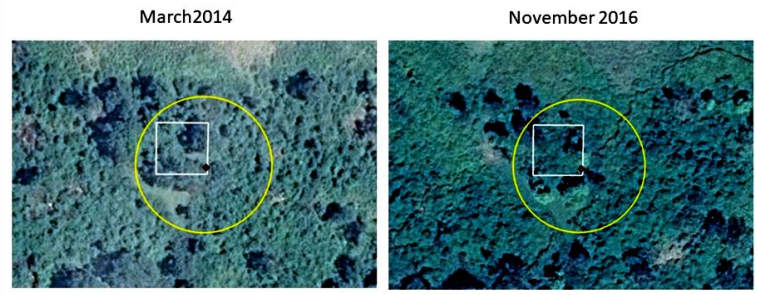

Figure 7: Google Earth images of test pixel (white square) and the corresponding area of change (yellow circle) of CBM observation (red points)

Analytically, the steps for the pixel-based approach are the following:

Firstly, we locate the SITS pixel corresponding to the CBM observation. Then pixel is assigned with the corresponding NF probability using the IDW function described previously. SITS data are deseasonalised to reduce dry forest seasonality and avoid false detection of deforestation. Then we create a CBM data stream of a single observation for the test pixel. Similarly, we create

a data stream for each sensor metric; Landsat NDVI, Sentinel-1 and PALSAR, incorporating all valid observations of the test pixel. At this point we can optimise the integration of CBM-SITS data streams. Final step involves the integration of data streams and detection of change by applying the Bayesian approach with the following parameters:

1. We use sensor specific pdfs of F/NF to calculate the conditional NF probability of each SITS observation. F/NF distributions are described using mean and standard deviation.
2. Set a threshold of deforestation probability at which flagged change is confirmed. Threshold identification was based on Reiche, Hamunyela, Verbesselt, Hoekman, and Herold (2018) results regarding Landsat, Sentinel-1 and PALSAR-2 spatial and temporal accuracy performance using different thresholds. Aiming for high confidence in area detection a mean threshold between 0.8 and 0.975 was used; $\chi \approx 0.9$.

Area-based approach

Pixel-based results indicate that Landsat NDVI is the only sensor metric that contributes on the detection of change. Therefore, area-based approach is applied between SITS (represented by Landsat NDVI) and CBM observations. The extent of the selected area covers all 17 CBM observations. Analytically, the steps are the following:

Firstly, we locate the SITS (Landsat NDVI) spatial points corresponding to the CBM observations and buffer them at an extent of equal size to the recorded area of change. All captured pixels in each area of change are extracted and assigned with NF probabilities using the IDW function described previously (fig.8). At this point we create 17 rasters by expanding each area of change to the desired extent. CBM rasters of similar recording date are then merged into a single layer. Similarly, single layers are finally merged into a CBM raster brick.

We crop SITS (Landsat NDVI) extent at the extent of CBM raster brick. Then SITS (Landsat NDVI) data are deseasonalised to reduce dry forest seasonality and avoid false detection of forest changes.

Using a forest mask derived from reference data from the beginning of the monitoring period, we can extract the forested pixels in order to isolate the areas of change. However, in our case there were no available reference data at the beginning of the monitoring period therefore forest mask derived from digitising a Google Earth image from March 2014. The date of the image is after the dry season of 2014 where most changes occur therefore we assume that only few deforestation events occurred until the beginning of the monitoring period; 2015.

Finally, the Bayesian deforestation detection approach is applied separately in all pixels of SITS (Landsat NDVI) and fused CBM-SITS data streams with similar parameters as with the pixel based approach. This creates the final deforestation maps.

5.2.3. Validation

The produced deforestation maps are divided into two strata: Change and No Change. Change represents the deforested area while No Change represents the remaining stable forest and stable non-forest area. The size of each stratum is calculated using pixel units.

The probability sampling design used is the stratified random sampling. The sample size is determined using the formula (no.13) from Olofsson et al. (2014) and calculation is presented in table 1. Based on Olofsson et al. (2014) approach, user accuracy of the No Change class is 0.9 and 0.95 for forest and non-forest stratum as stable classes are known to be more accurate, while for the Change class 0.7. The target standard error for overall accuracy is 0.01.

As presented in table 1, the number of samples based on the total area is 760. Due to the very small proportion of Change class, samples are distributed by allocating a minimum sample size of 150 to adequately sample this strata. However, in order to ensure the assessment of the CBM data streams contribution to the Bayesian approach, from 150 samples of change stratum a minimum sample size of 50 is allocated similarly to the CBM areas. The rest are distributed proportionally to the No Change class; stable forest and non-forest. Since non-forest stratum was not covered during the production of change maps it is excluded and only forest stratum will be compared. Therefore, the final number of samples is 291.

	Change		No Change		Total
			Stable F	Stable NF	
Area in pixels	2992		3099	10757	16848
Wi (Mapped proportion)	0.18		0.18	0.64	
Ui (Expected user's accuracy	0.7		0.9	0.95	
Si (Standard deviation)	0.46		0.3	0.22	
*Wi*Si*	0.08		0.05	0.14	0.27
			SE overall accuracy		0.01
			Number of samples		760
	Sample size per stratum				
Allocation	150		141	469	760
Divide change stratum	CBM change areas	Rest change areas	Stable F	Stable NF	
Final allocation	50	100	141	469	760
Exclude stable NF stratum	50	100	141	-	291
			Final number of samples		291

Table 1: Sample size calculation and allocation per stratum based on Olofsson et al. (2014)

Subsequently, the strata are randomly sampled. The output is a CSV file containing the cell number and coordinates of each sample.

Reference data are created by analysing the time series signal of each sampling pixel both from SITS (Landsat NDVI) and CBM-SITS produced deforestation maps. For spatial accuracy assessment the analysis involves the confirmation of change or no change at each sampling pixel. Subsequently, spatial accuracy measures derive from the error matrix of Change and No Change class and include the overall accuracy (OA), user's accuracy (UA) and producer's accuracy (PA). For temporal accuracy assessment the analysis involves the identification of the reference deforestation date. To avoid imprecision, reference deforestation date is identified as the date right in-between the acquisition date of the first image of the deforestation event and the previous (Reiche et al., 2018). Temporal accuracy assessment is based on the time-difference between the

confirmed and reference deforestation date of each sampling pixel; mean-time-lag (MTLc). In addition, the mean time lag of the date at which the confirmed deforestation events were initially flagged (MTLf) was calculated.

6. Results

This section comprises the (i) F/NF separability analysis results of SITS (research question 1, method 4.2.1), (ii) pixel and field based results of the CBM-SITS deforestation detection approach (research question 2, method 4.2.2) and (iii) the spatial and temporal accuracy results of SITS and CBM-SITS integration-approach (research question 3, method 4.2.3).

6.1. F/NF Separability analysis

Signature analysis results for each data stream can be seen at figures 8-10 and include the mean, standard deviation and the backscatter or NDVI signal of F and NF class.

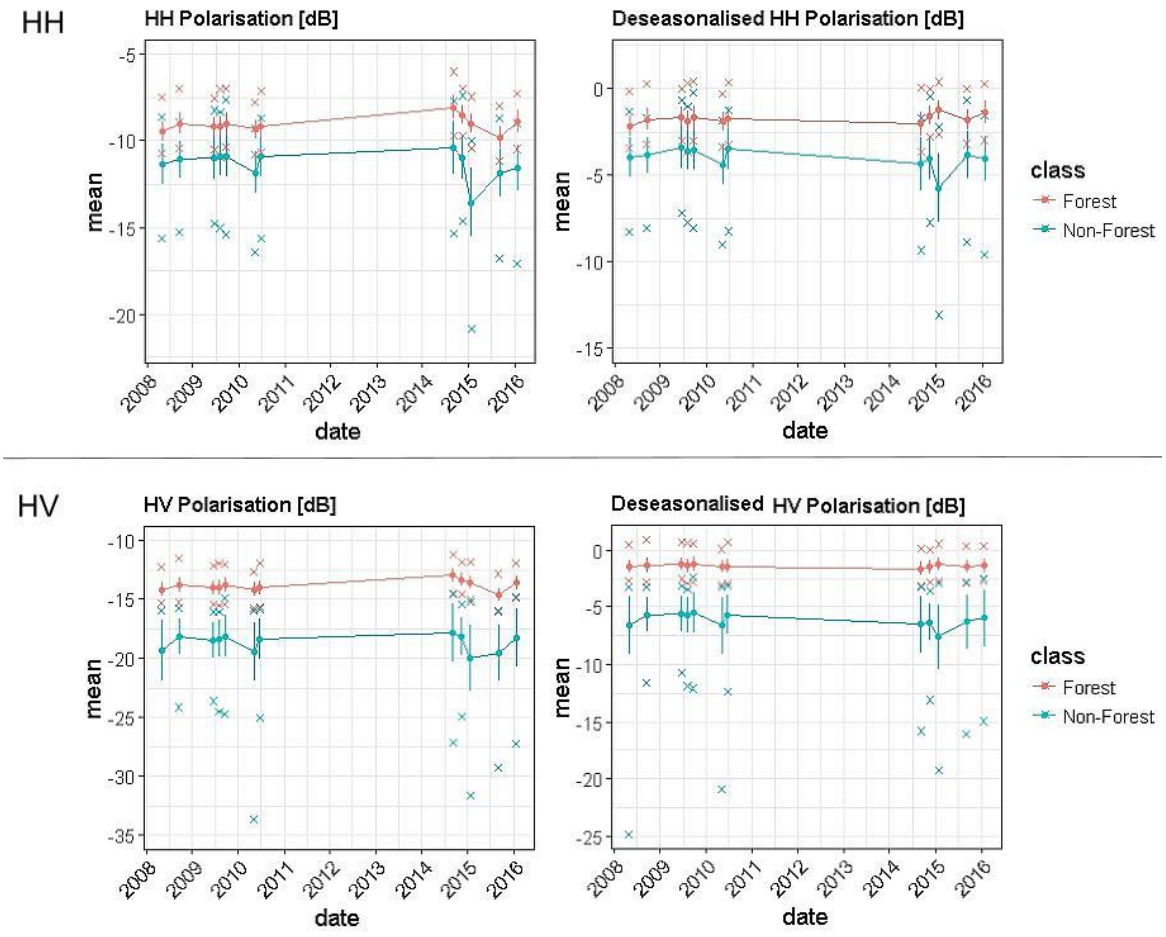

Figure 8: Annual HH and HV backscatter characteristic of the original and deseasonalised PALSAR time series. Red line indicates forested areas - blue line indicates non-forested areas. Vertical lines at each observation depict the standard deviation from the mean

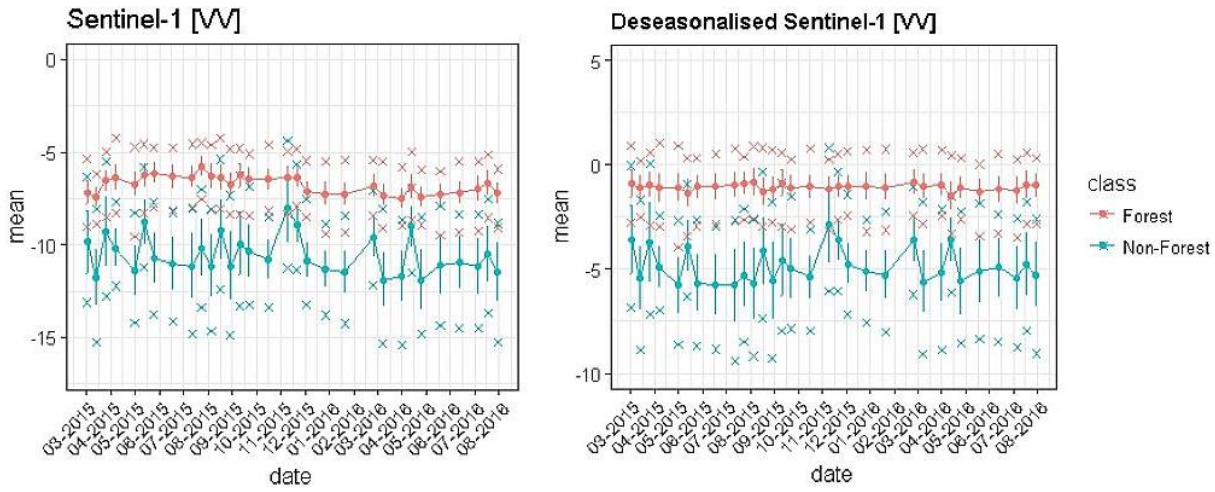

Figure 9: Monthly VV backscatter characteristic of the original and deseasonalised Sentinel-1 time series. Red line indicates forested areas - blue line indicates non-forested areas. Vertical lines at each observation depict the standard deviation from the mean.

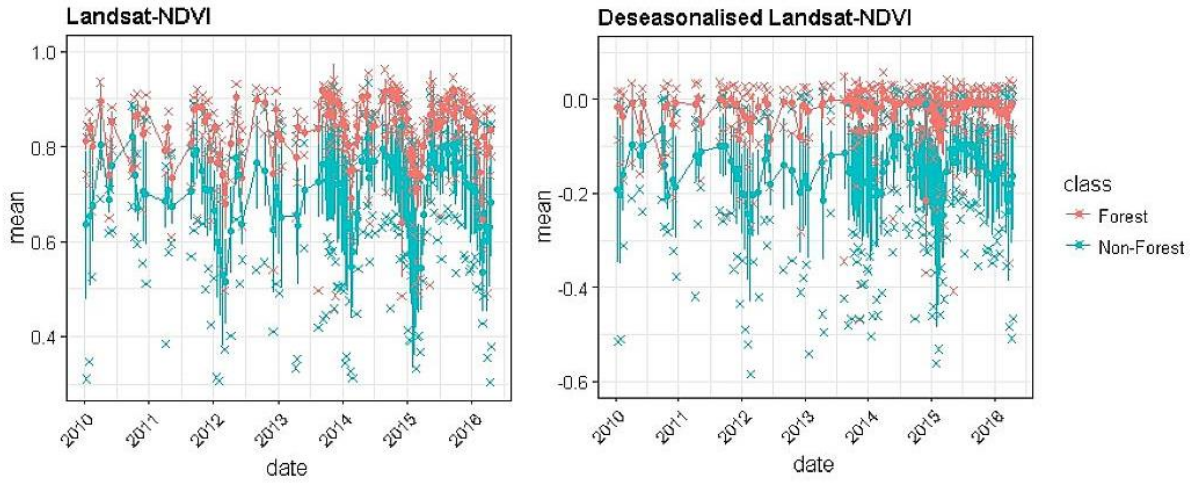

Figure 10: NDVI values of the original and deseasonalised Landsat time series per year. Red line indicates forested areas - blue line indicates non-forested areas. Vertical lines at each observation depict the standard deviation from the mean

Separability analysis results were based on the JM distance between F and NF classes. A summary of the JM results can be seen in table 2 where PALSAR HV indicates the best performance while Landsat-NDVI the poorest.

	JM		
SITS	Original	Deseasonalised	Performance
PALSAR HH	0.88	0.97	3
PALSAR HV	1.47	1.54	1 (best)
Sentinel-1	1.36	1.49	2
Landsat-NDVI	0.55	0.89	4 (poorest)

Table 2: Separability analysis results based on JM distance between F and NF classes for each satellite image time series (SITS); original and deseasonalised.

6.2. Integration of CBM-SITS data streams

Application of the Bayesian deforestation detection approach requires the prior conversion of SITS and CBM observations into conditional F/NF probabilities. Then, the proposed integration approach is tested in a single pixel to evaluate the integration of CBM-SITS data streams; before applied in all pixels of the study area (area-based approach).

Derive F/NF pdfs

Derivation of F/NF pdfs for each deseasonalised SITS data stream are presented in fig. 11. F/NF distributions of PALSAR and Sentinel-1 appear more separate than Landsat's NDVI data stream.

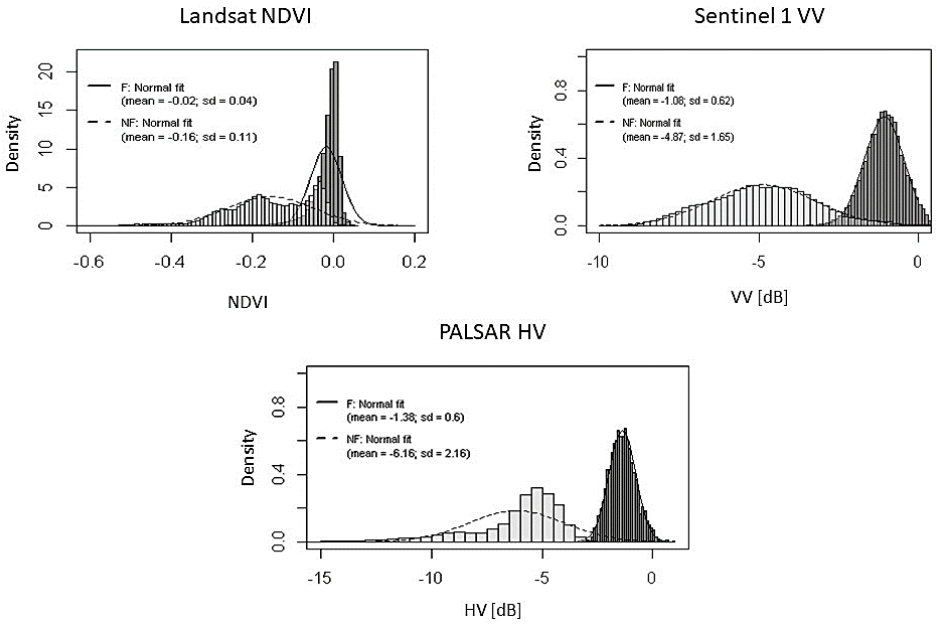

Figure 11: Forest (F) and non-forest (NF) distributions overlaid with probability density functions (pdfs) fitted separately for the deseasonalised SITS data streams

Pixel-based approach

Method is tested first in a single pixel to evaluate the integration of CBM-SITS data streams; results are presented in fig.12.

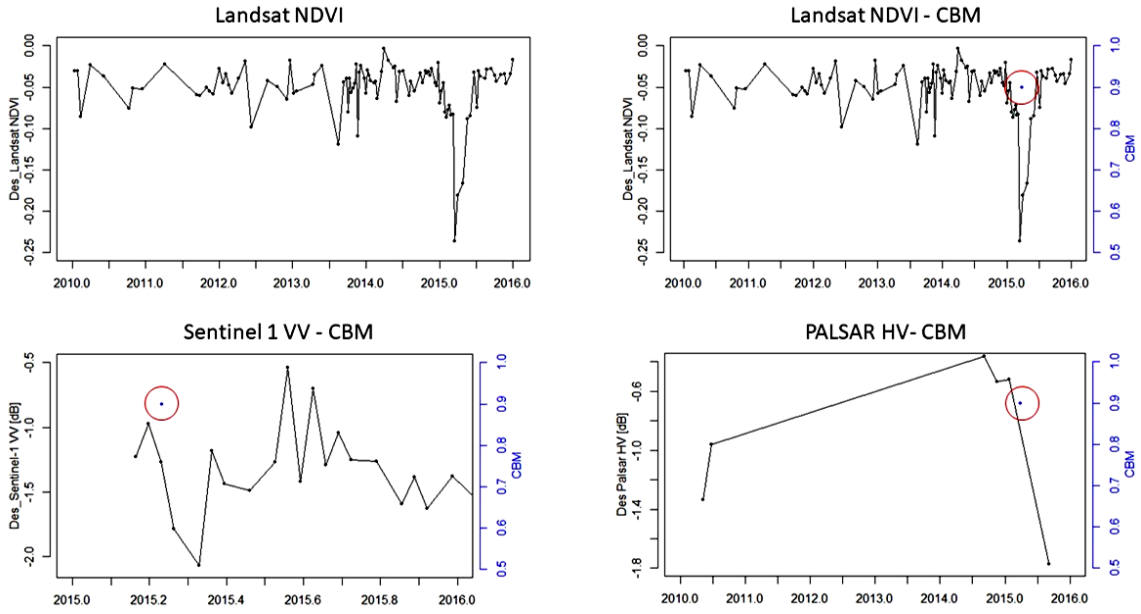

Figure 12: CBM and SITS data streams covering a deforestation event in early 2015. red circle = CBM observation

Application of the Bayesian deforestation detection approach using a high threshold of deforestation probability at which flagged changes are confirmed; $\chi = 0.9$. For better optimization of detected deforestation events length of data streams reduced to the range 2014-2016, with 2015 being the start of the monitoring period (fig. 13 – 15).

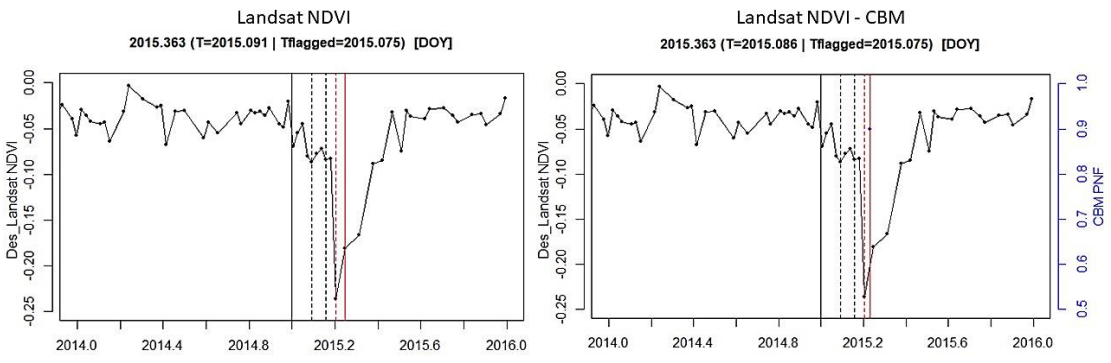

Figure 13 Landsat NDVI and CBM data streams and detected deforestation events. black line = start of monitoring; dotted black line = flagged deforestation event that was not confirmed; red dotted line = flagged deforestation event; red line = confirmed deforestation event; Tflagged= day deforestation event flagged; T= day deforestation event confirmed

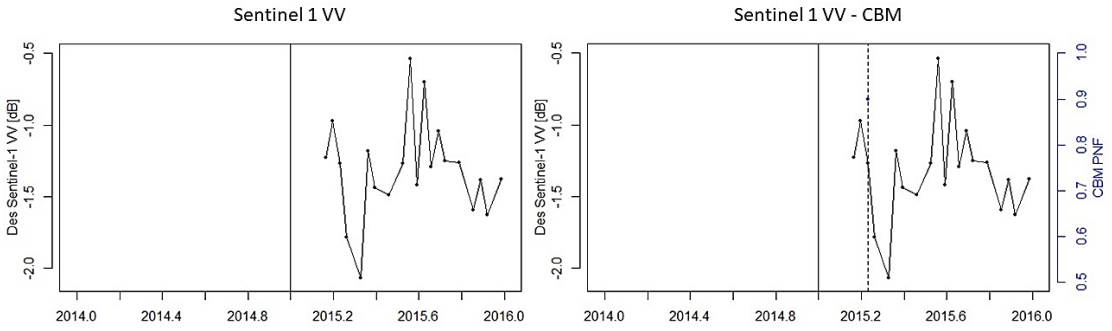

Figure 14: Sentinel-1 and CBM data streams and flagged unconfirmed deforestation event. black line = start of monitoring; dotted black line = flagged deforestation event that was not confirmed;

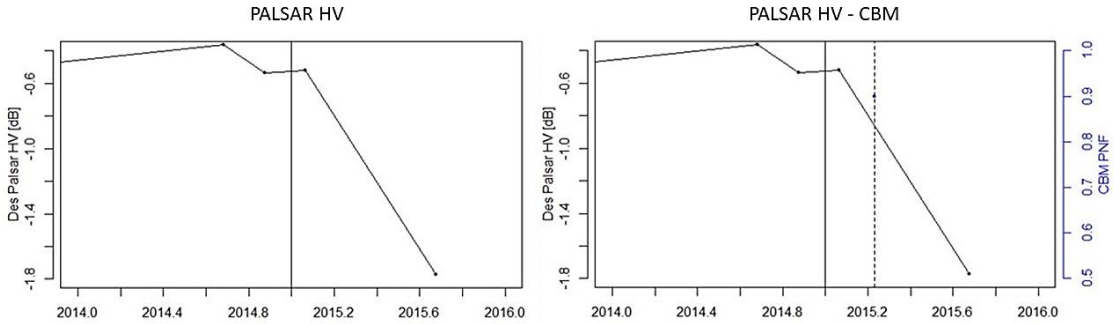

Figure 15: PALSAR HV and CBM data streams and flagged unconfirmed deforestation event. black line = start of monitoring; dotted black line = flagged deforestation event that was not confirmed;

Area-based approach

Prior to the application of the Bayesian deforestation detection approach in all pixels of the study area, we firstly derive NF probabilities (PNF) from CBM observations. An example is depicted in fig. 16.

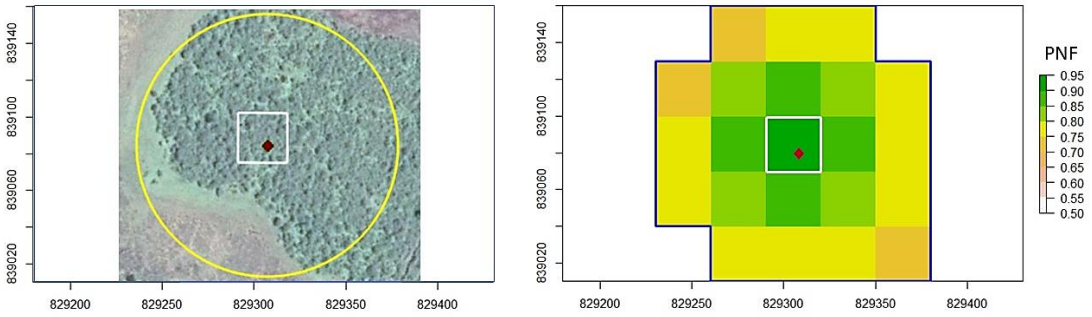

Figure 16: Example of converting a CBM observation (left) into NF probabilities (PNF) (right); red point= CBM observation; white square= corresponding raster pixel; yellow circle= recorded *area of change*

The CBM raster data stream consists from all converted observations into PNF (fig. 17).

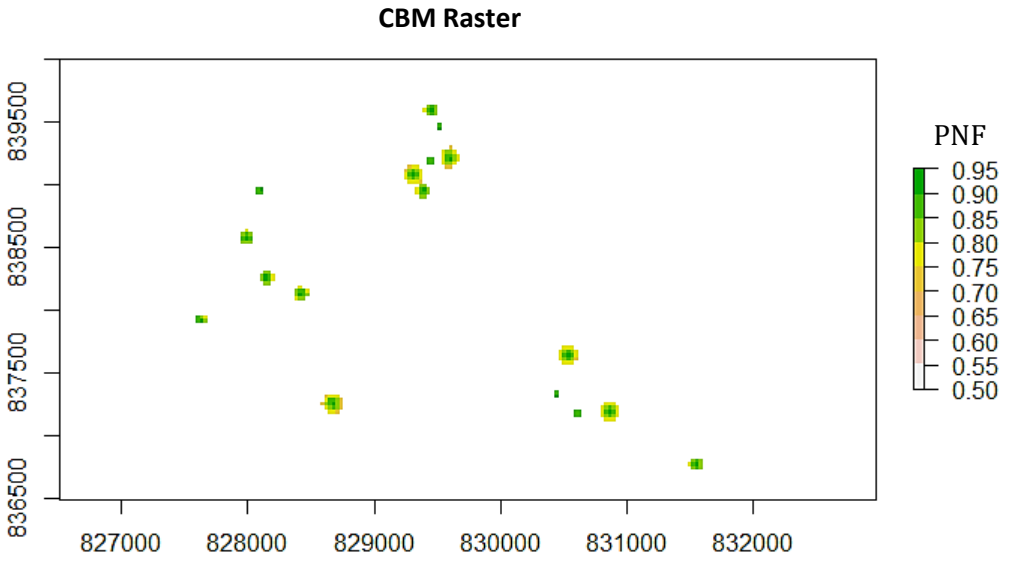

Figure 17: Creation of CBM raster data stream incorporating all converted observations into NF probabilities (PNF)

Stable NF areas are excluded from both SITS (Landsat NDVI) and CBM data streams using stable forest mask from reference data (fig. 18).

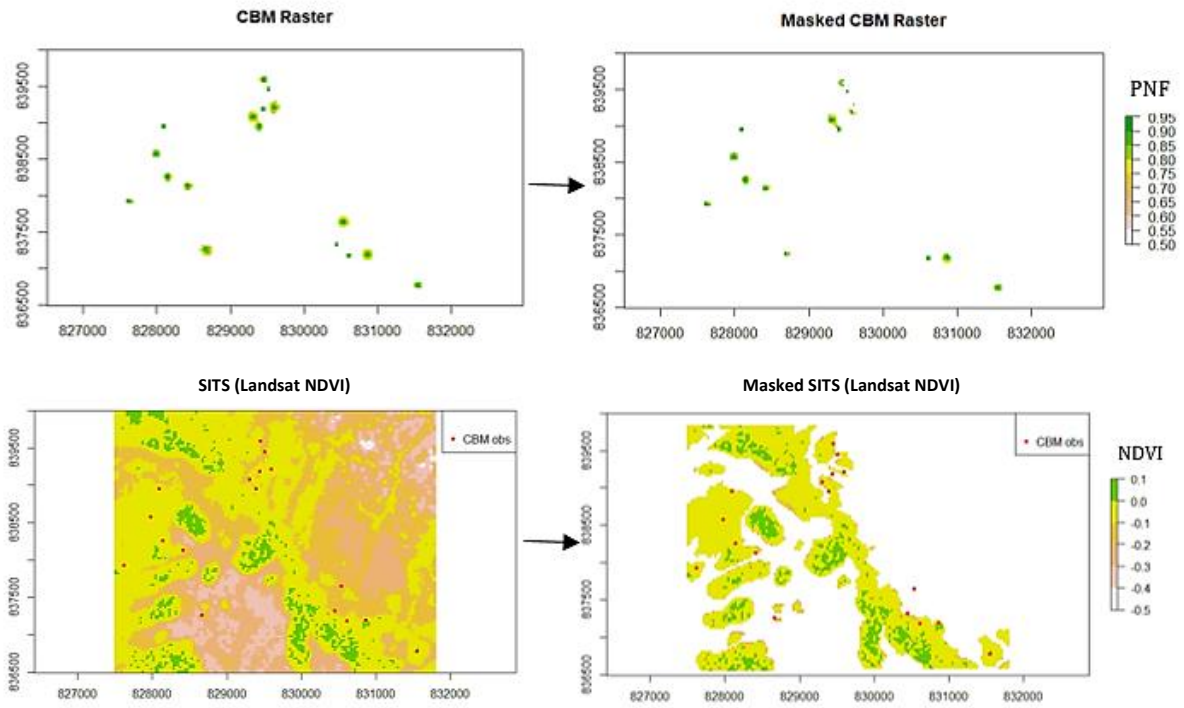

Figure 18: Masking CBM and SITS (Landsat NDVI) data streams using a stable forest mask

Application of the Bayesian deforestation detection approach for SITS (Landsat NDVI), and CBM-SITS and production of deforestation maps (fig. 19).

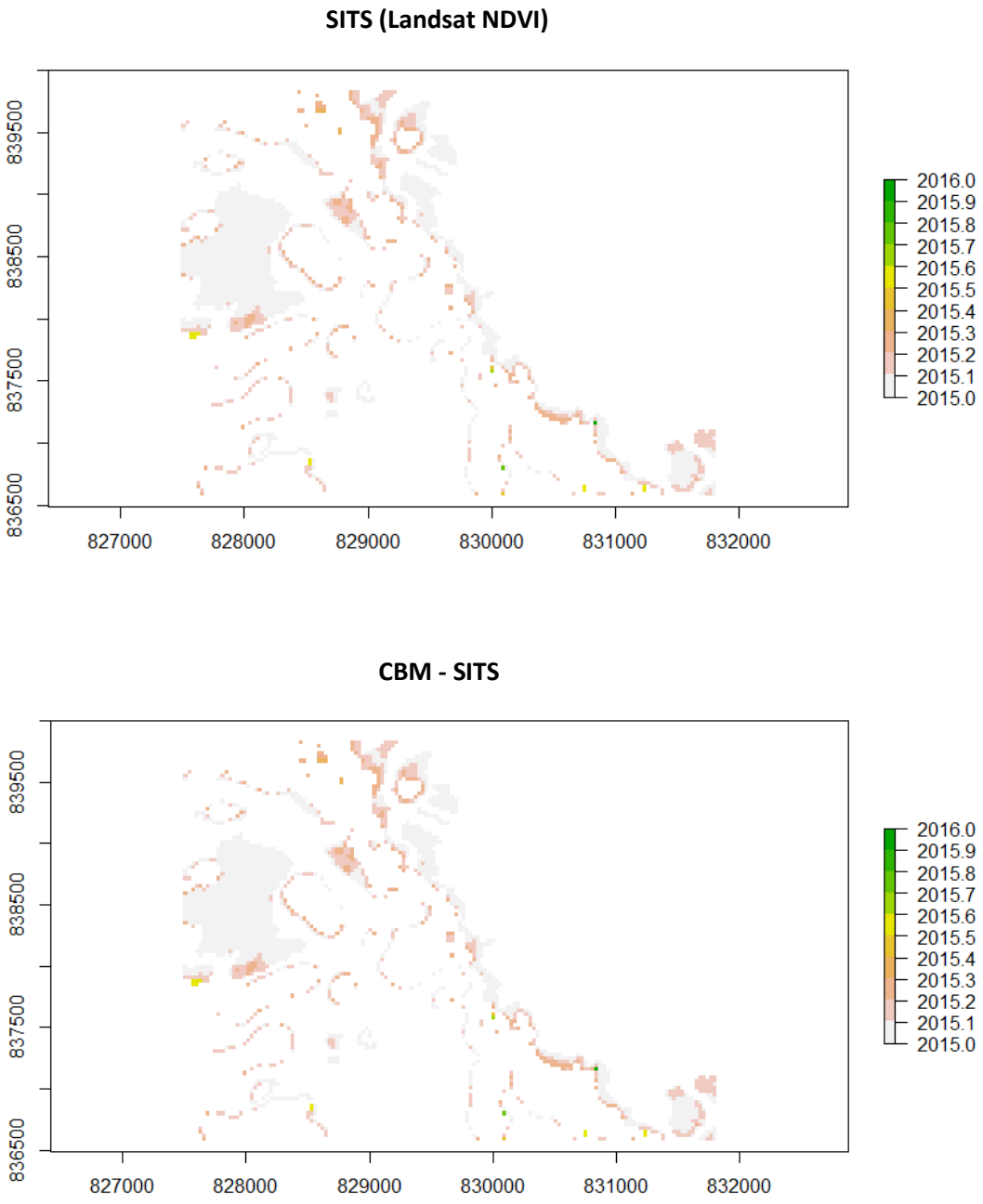

Figure 19: SITS (Landsat NDVI) and CBM-SITS produced deforestation maps

6.3. Spatial and temporal accuracy assessment

Accuracy assessment results are based on the comparison of SITS (Landsat NDVI) and CBM-SITS produced deforestation maps with reference data.

Spatial accuracy assessment results are presented in table 3.

Reference

Map / Classes	*Change*	*No Change*	**Total**
Change	149	0	149
No Change	1	141	142
Total	150	141	291

SITS

User's Accuracy (UA)
Change: 99.33% ------ CE= 0.66 %
No Change: 100% ---- CE= 0 %
Producer's Accuracy (PA)
Change: 100% --------- OE= 0 %
No Change: 99.30% -- OE= 0.6 %
Overall Accuracy (OA): 99.65 %

Reference

Map / Classes	*Change*	*No Change*	**Total**
Change	150	0	150
No Change	0	141	149
Total	150	141	291

CBM - SITS

User's Accuracy (UA)
Change: 100% --------- CE= 0 %
No Change: 100% ----- CE= 0 %
Producer's Accuracy (PA)
Change: 100% --------- OE= 0 %
No Change: 100% ----- OE= 0 %
Overall Accuracy (OA): 100 %

Table 3: Spatial accuracy assessment of SITS (Landsat NDVI) and CBM-SITS

Temporal accuracy assessment results are presented in table 4.

Temporal accuracy assessment	**Change Maps**			
	SITS		**CBM-SITS**	
	flagged	confirmed	flagged	confirmed
Mean-Time-Lag (days)	0.14	13.17	0.137	13.06

Table 4: Temporal accuracy assessment of SITS (Landsat NDVI) and CBM-SITS

7. Discussion

F/NF separability analysis

In signature analysis results of PALSAR and Sentinel-1, backscatter characteristics of forested areas appear relatively stable along the original time series (fig. 8 & 9). This indicates the high contribution of forest-canopies structural characteristics in the total backscatter signal. Nevertheless, dielectric characteristics of forest canopies and soil appear to have also an impact on backscatter as a result of C and L-band sensitivity to vegetation and soil water content. Specifically, comparison of climatic data of the region (fig.20) with the backscatter signal (fig. 9 & 10) indicates that low rainfall in January corresponds with low backscatter while high rainfall in August with high backscatter values. In general, seasonal changes correspond roughly with low backscatter for dry season (December-February) and high backscatter for the main wet season (June-August).

On the other hand, Landsat-NDVI values due to their relation with the photosynthetic capacity of plants are strongly influenced by seasonal variations in climate. Therefore, high photosynthetic activity during the growing season (wet season) corresponds with high NDVI values. However, in fig. 10 we can observe that NDVI values remain relatively high until the first half of the dry season (January). This shows that photosynthetic activity can be maintained in high levels during the dry season, depending on the water storage held from wet season. Guan et al. (2015) has calculated that tropical rainforests worldwide with an annual rainfall threshold of approximately 2,000 mm yr−1, water availability can preserve the evergreen state during dry season. Kafa reserve has a mean annual rainfall between 1700 and 1900 mm (Riechmann, 2007), which validates that water storage can maintain the photosynthetic activity in high levels for a part of the dry season. From the above mentioned, we can also certify the relation between NDVI and rainfall. Comparing the original NDVI values (fig. 10) with the average rainfall data from the area (fig. 20) we can observe that high rainfall during the wet season (June-August) increases photosynthetic activity and therefore the NDVI values, while the opposite occurs during the dry season..

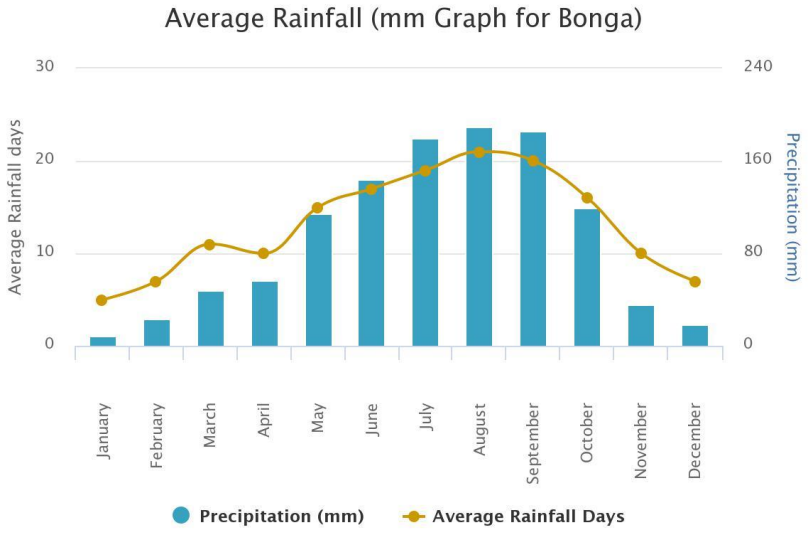

Figure 20: Average rainfall data of nearest meteorological station to Kafa reserve (www.worldweatheronline.com)

In order to isolate the influence of seasonality from our independent backscatter and NDVI variables, optical and SAR SITS have been deseasonalised using spatial context. Previous study has shown that spatial context approach improves the early detection of forest disturbance in areas with strong seasonality (Hamunyela et al., 2016). In addition, the reduction of seasonal variation from the original data, except of providing a safer path to compare two or more time series, has also improved the separability of F and NF classes.

After time series data being deseasonalised, JM distance between F and NF distributions increased significantly (Table 2). PALSAR HV indicates the best performance with JM distance of 1.54. This is due to volume scattering that generates a contrasting HV backscatter signal, higher for forests and lower for non-forests, which improves the detection and separability of the classes. The 2014 newly launched Sentinel-1 satellite, gives an almost equal performance with JM distance of 1.49. Little research has been done on the significant potential of Sentinel-1 however due to the C-band SAR a lesser performance was expected on distinguishing the two classes. The combination of Sentinel-1 C-band SAR separability performance and density of observations promises to be a particular useful tool for forest change detection. On the other hand, HH time series performance depicts more overlap between F/NF classes as indicated by the JM distance (0.97). HH performance is usually less than HV due to its strong interaction with horizontal branches and weak double bounce scattering. Finally, Landsat-NDVI shows the poorest results (JM=0.89) as it can receive similar signal from evergreen forests and low vegetation such as, grass and small bushes. Therefore, it is difficult to distinguish the classes as clear as radar systems.

F/NF pdfs

Derivation of F/NF pdfs is the first and most important part of the Bayesian approach (fig. 11). Based on F/NF distributions data stream observations are converted into deforestation probabilities and therefore confirm or reject a deforestation event at the image acquisition days (Reiche, 2015). Pdfs are area-specific; different study areas require re-calculation of pdfs. While this can be a limitation, on the other hand, area-specific pdfs remain stable over time and no re-calculation is needed. This allows a long range deforestation detection monitoring over stable areas.

Threshold of deforestation probability

In this research we use a high threshold of deforestation probability at which forest changes are confirmed; χ=0.9. This is to avoid false detection of change and low intensity deforestation events; forest degradation, which is not covered in this thesis. High thresholds expect to increase SITS spatial accuracy, produce quality deforestation maps and provide low area bias (Reiche et al., 2018). Deforestation maps of high spatial accuracy will ensure the detection of pixels corresponding to CBM observations, to properly assess the integration approach and the CBM contribution.

Pixel-based approach

Test pixel results indicate the high contribution of Landsat NDVI on deforestation monitoring. This is due to the high density of valid observations that provide information in short time intervals. However, this was not the case with Sentinel-1 and PALSAR.

Landsat's valid observations start from 2010 until the end of the monitoring period providing a rich history of NDVI signal . For the test pixel's monitoring period, optimization of Landsat's NDVI data stream shows a clear deforestation event at the end of March (fig. 12). After integrating Landsat NDVI with CBM data stream CBM observation appears to be recorded during the deforestation event (fig. 12). Application of the Bayesian change detection approach confirms the previous visual interpretation of data streams. Using a high threshold of deforestation probability at which forest changes are confirmed, Landsat single-sensor approach capture change on the 1th of April while Landsat-CBM multi-sensor approach capture change on the 27th of March (fig. 13). This is a clear indication of the contribution of CBM observations on early deforestation detection. In this case, CBM observation improved the deforestation detection 5 days earlier than with Landsat single sensor approach.

On the other hand, Sentinel-1 data stream observations start late, on March, barely covering the beginning of the pixel's deforestation event and doesn't provide any change detection (fig. 14). Integrating Sentinel-1 with CBM, flags a change at the date of CBM observation which cannot be confirmed as it is not supported with high PNFs from past and future radar observations (fig. 15). Taking into account that test pixel represents the latest detected deforestation event from all CBM observations Sentinel-1 contribution on change detection is not expected. For this reason Sentinel-1 is excluded from the area-based approach.

Similarly, PALSAR provides only two observations in the monitoring period, from which none is within the period of the pixel's deforestation event and only one is within the dry season where most deforestation events occur (fig. 15). Therefore it is also excluded from the area-based approach.

Area-based approach

Based on pixel-based results, area-based approach applied using SITS (Landsat NDVI) and CBM data streams.

Basic core of the area-based approach is the conversion of CBM observations into NF probabilities. Parallel to the conversion, CBM recordings were evaluated and the following problematic cases revealed:

Incomplete CBM recordings: In this research we assume that forest rangers are standing at the center of deforested areas therefore applied a circular buffering to capture the areas of change. Forest rangers also give an estimation of the area of change based on which we can identify the radius of circular buffering. However this was not the case for all observations. As we can see in fig.21, forest ranger is standing at the edge of a deforestation event and not at its center. As a consequence, forest ranger's recording regarding the estimated area of change is directional, from his position to the north-east, something that cannot be predicted and does not go along with the proposed circular-buffering approach. In this case, almost half of circular buffering

captures the stable NF area while the other half a fraction of the actual deforested area. This situation along with inaccurate estimations of the area of change was the case for almost half of CBM observations decreasing the actual extent of deforestation events.

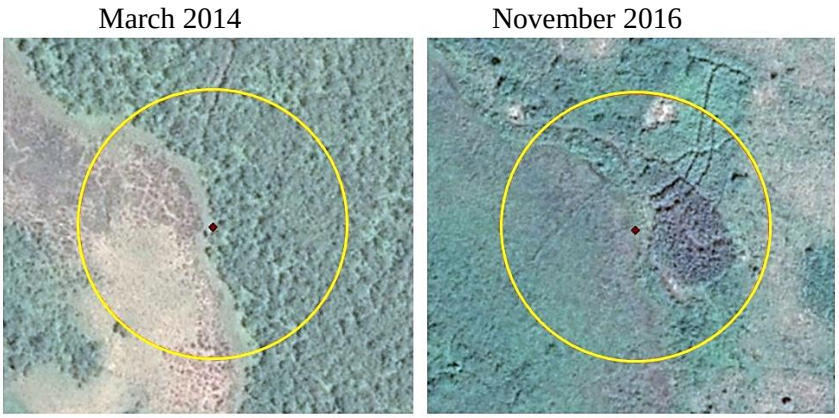

Figure 21: Google Earth images of an incomplete CBM recording; red point= forest ranger's standing point; yellow circle= circular buffering representing ranger's estimated *area of change*

Delayed CBM recordings: Application of the Bayesian approach using SITS (Landsat NDVI) dense data stream in all pixels corresponding to CBM observations indicated that almost half of them were flagged and confirmed right-at-the-beginning of the monitoring period (fig.22). Specifically, most deforestation events either occurred at the beginning of the monitoring period, January, or even before. On the other hand, CBM observations were recorded on three different dates within March. Therefore they have a recording delay of 3 months which is not expected to provide any contribution on deforestation detection.

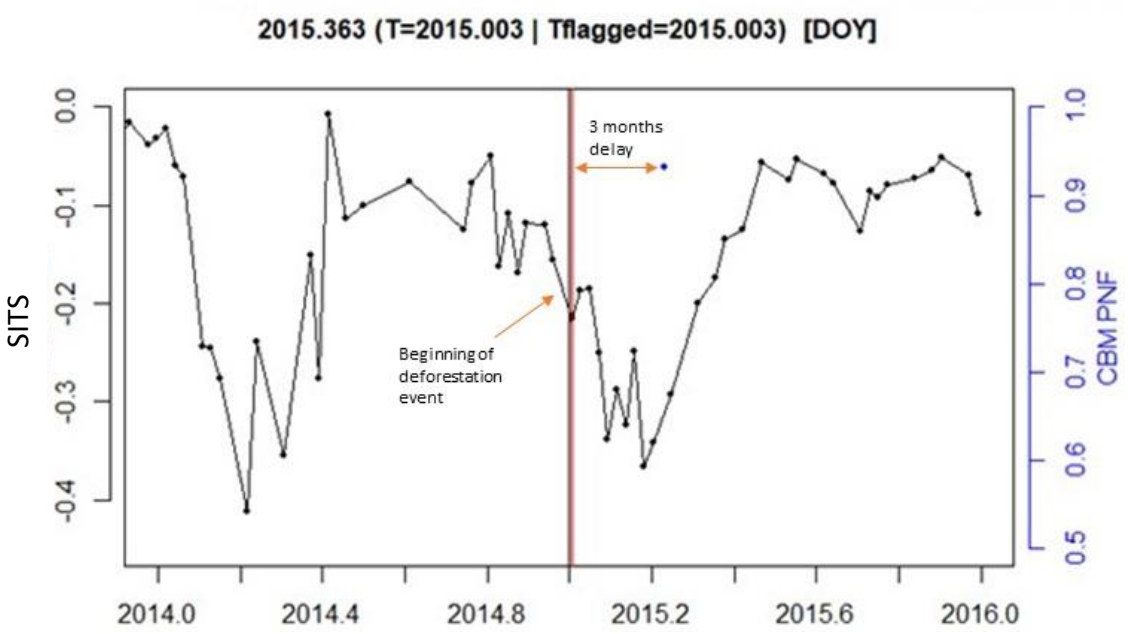

Figure 22: Example of a 3 month delayed CBM recording; black line = start of monitoring; red line = confirmed deforestation event; Tflagged= day deforestation event flagged; T= day deforestation event confirmed

False CBM recordings: Two CBM observations are located at stable NF areas where there is no deforestation. However, these CBM observations and recorded areas of change were automatically deleted after masking with stable forest reference data.

Subsequently, converted observations were joined for the creation of CBM raster data stream (fig. 17). Comparison of CBM raster with produced deforestation maps (fig. 19) shows that converted areas represent a tiny part of the total detected deforested area; 6.3%. In greater extent this is likely a result of deficient community-based monitoring while in smaller extent a cause of incomplete recordings. After masking CBM raster with stable forest mask (fig. 18) converted areas are further reduced to just 4.5% of the total deforested area. This drop is a consequence of the incomplete and false recordings described previously. The general decrease of pixels reduces accordingly the potential contribution of CBM data stream on the deforestation detection approach.

The impact is visible in the produced deforestation maps of SITS (Landsat NDVI) and CBM-SITS (fig. 19) which, in first sight, show identical spatial and temporal allocation of changes. However, deforestation maps of single and multi-sensor approach use a colour palette of 10 separate colours to represent the detected deforestation dates in 10 periods of 36.5 days (1/10 of the total annual days). Therefore, the actual time of change within the periods may vary between the approaches and a temporal accuracy assessment, along with a spatial, is needed.

Spatial and temporal accuracy

The spatial and temporal accuracies of the multi-sensor CBM-SITS approach were barely higher when compared to those of single sensor SITS (Landsat NDVI) approach (table 3-4). The minimum contribution of CBM observations is a result of their low density and mostly, their delayed recording compared to the period most deforestation events occur.

Specifically, CBM contribution presented in just one sampling pixel of a late deforestation event; March (fig. 23). At this sampling pixel CBM-SITS approach confirms a deforestation event based on a CBM observation, while SITS (Landsat NDVI) approach does not confirm any change (fig. 23). In the latter case sampling pixel is treated as commission error. As a result, the UA of the Change class, single to multi-sensor approach, increases from 99.33% to 100% and the OA increases from 99.65% to 100%. High spatial accuracies from both approaches is a result of SITS (Landsat NDVI) observation density and the high threshold used, $\chi = 0.9$, at which forest changes are confirmed, significantly limiting false detection of change and degradation events. However, spatial accuracies are too high to be realistic. This can be a result of the small sampling size used thus, an alternative sampling design should be considered.

During the temporal accuracy assessment of SITS (Landsat NDVI) approach, sampling pixel was excluded from the calculation of MTLc as no change detected (fig. 23). As a result, the MTLc of SITS (Landsat NDVI) approach appears almost equal with the MTLc of CBM-SITS approach (table 4) while actually has a slightly less performance. However, since there is no scientific way to penalize "temporally" the inability of a sampling pixel to detect change, results from both approaches appear similar. Such cases may introduce inaccurate information to the assessment and should be considered. In general, temporal accuracy results appear higher compared to previous study (Reiche et al., 2018) providing an MTLc of approximately 13 days (table 4). CBM contribution is barely higher than SITS (Landsat NDVI); -0.12 MTLc. This is a result of SITS

(Landsat NDVI) high density of valid observations over the deforestation period which provides change-information in short time intervals. However the instability of SITS (Landsat NDVI) to provide stable performance over time, due to persistent cloud cover over the tropics, should be considered.

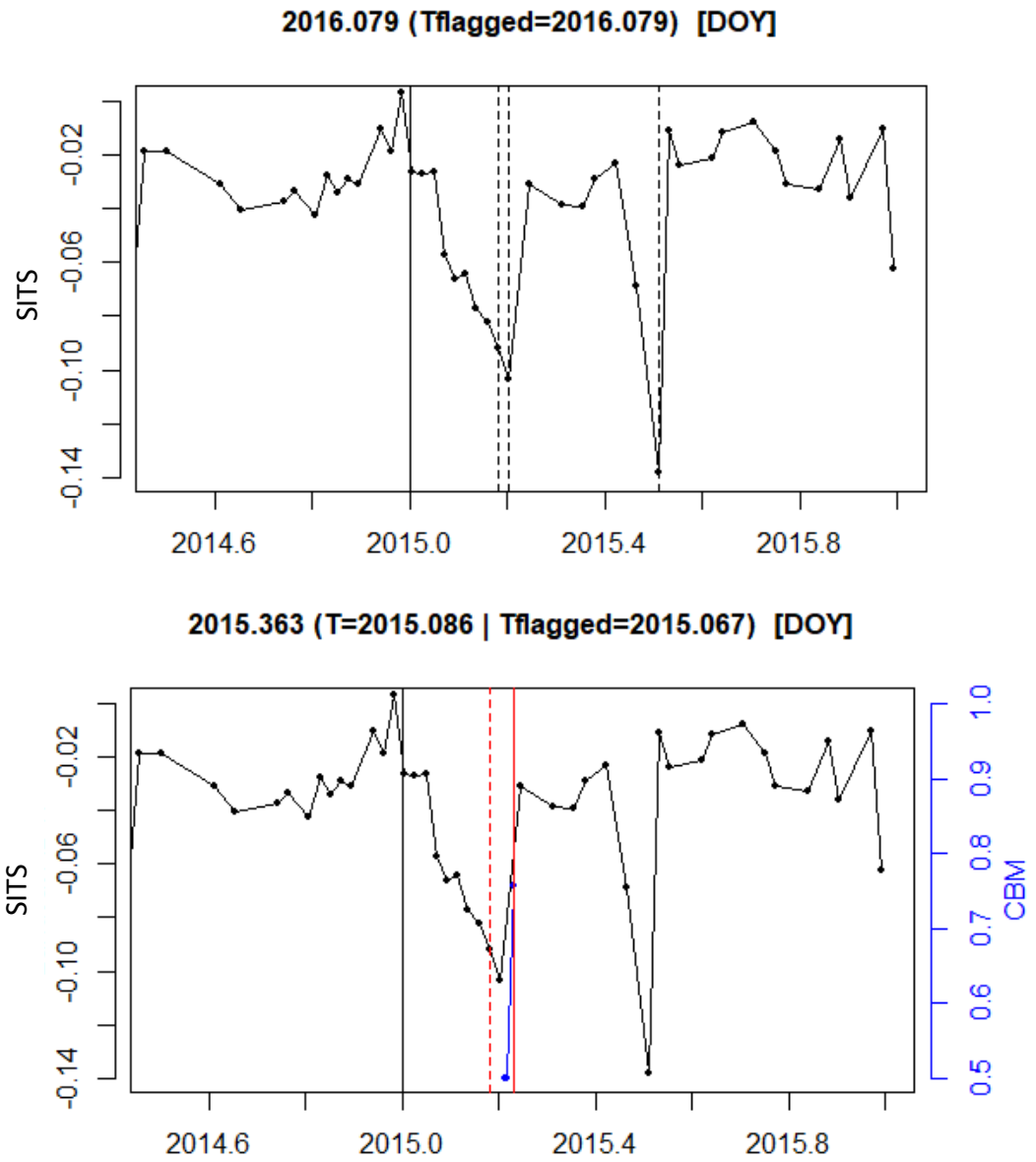

Figure 23: (top to bottom) SITS (Landsat NDVI) and CBM-SITS data streams, and detected deforestation events in a single sampling pixel. black line = start of monitoring; dotted black line = flagged deforestation event that was not confirmed; red dotted line = flagged deforestation event; red line = confirmed deforestation event

On the other hand, the mean time lag of the dates at which deforestation events were initially flagged (MTLf) appears almost identical with the reference dates presenting a time difference of approximately 0.14 days for both sensors (table 4). The significantly high temporal accuracy of SITS (Landsat NDVI) flagged deforestation events indicate rapid detection of change. This is a result of the low threshold used for flagged events, χ =0.5, which is confirmed by previous study (Reiche et al., 2018) to present high temporal accuracies.

8. Conclusions

The objective of the thesis is to build upon an existing probabilistic (Bayesian) approach to combine CBM with SITS data streams for NRT deforestation detection in Kafa, Ethiopia.

Application of the proposed integration method in a single pixel indicated the efficiency of the Bayesian approach to incorporate converted CBM observations and correctly derive timely information of deforestation events. Particularly, CBM observations improved the detection of change 5 days earlier than with SITS (Landsat NDVI) single sensor approach. However, the overall contribution of CBM observations over the area was minimum (+0.35% OA, -0.12 days MTLc) as a result of their low temporal density and mostly, their delayed recording compared to the period most deforestation events occur. Consecutively, CBM data show high potential for contribution on early deforestation detection if only the recordings are frequent providing high density of observations over the study area.

Due to the minimum contribution of CBM data, spatial and temporal accuracy results reflected mainly SITS (Landsat NDVI) performance. Results indicated that high thresholds of deforestation probability at which forest changes are confirmed provide high spatial accuracy and can be used to detect deforested pixels. On the other hand, lower thresholds of deforestation probability at which forest changes are flagged provide high temporal accuracy and can be used to detect deforested dates at corresponding pixels. Simultaneous application of the above thresholds into the Bayesian framework promises to increase significantly both the spatial and temporal accuracy of SITS data streams.

For SITS, three factors play determining role on deforestation detection monitoring: F/NF separability, observation density and observation coverage over deforestation period. ALOS PALSAR shows high F/NF separability, however due to its low temporal density provided just a single observation over the deforestation period. Sentinel-1 showed high F/NF separability and observation density, however observations did not cover the deforestation period. On the other hand, while Landsat NDVI showed the lowest F/NF separability among sensors, it provided high density of valid observations over the deforestation period. As a result, Landsat NDVI was the dominant sensor for deforestation detection monitoring in this research. Overall, while the identification of the sensor metric with the higher sensitivity capability to detect deforestation is important (F/NF separability), observation density and observation coverage over deforestation period are priority factors.

9. Recommendations

Based on the findings of this research, for the establishment of an efficient deforestation monitoring system that incorporates CBM and SITS observations the following are recommended:

For CBM data:

- *Consistent monitoring over the study area to avoid delayed recordings*: This requires a strategic planning for i) surveying the area, ii) human resources and iii) training forest rangers. Strategic planning should also take into consideration field survey limitations;

weather conditions, inaccessible areas etc. Main focus of consistent monitoring should be the frequency of data acquisition over the study area.

- *Recording position and area of change estimation*: Forest rangers should be aware of the methodology and position themselves at the center of deforestation events. Instead of estimating the area of change in hectares (ha), which is based on personal perception, a better approach could be to estimate the maximum radius of change in meters or feet. Deforestation events that extend to NF areas are no problem since masking with stable forest reference data will automatically delete them. Deforestation events that extend to F areas can be excluded by masking with high quality SITS deforestation maps. Deforestation maps of high spatial accuracy can be produced using high thresholds of NF probabilities at which forest changes are confirmed; 0.9. Other approaches of area estimation involve; mapping the boarders or recording the four corners of deforestation events. However, these approaches can be more time consuming.

For SITS data:

- *High F/NF separability*: The sensitivity capability to discriminate F/NF classes is important for deforestation detection.
- *High temporal density of observations over the deforestation period*: This will provide change-information in short time intervals for early deforestation detection.
- *Consideration of optical sensors performance*: Optical images are dependent on the absence of clouds in the tropics which can decrease significantly the total number of valid observations. Moreover, valid observations can be distributed unequally over forest areas increasing the uncertainty for a stable deforestation detection performance. These factors should be considered and a cloud cover assessment of the monitoring areas can be indicative for optical sensors expected level of performance.
- *Consideration of SAR sensors performance*: SAR sensors may provide a safer and more stable approach than optical sensors as they provide a high number of valid observations equally distributed over areas. In particular, Sentinel-1 data streams show high F/NF separability while the re-visit time of both constellations, A and B, can provide observations every 6 to 12 days. In this case, the cross-polarisation channels of Sentinel-1 are recommended as they have shown to be more effective in agricultural mapping and crop monitoring (Notarnicola et al., 2017). However, there is little knowledge on the capabilities of Sentinel-1 for forest change monitoring (Reiche, 2015) and further research is needed.

For reference data:

- *Deriving a reliable stable forest mask:* Using a stable forest mask derived from reliable reference data, we can extract the forested pixels and isolate the areas of change. Forest mask is advised to derive at the beginning of the monitoring period from different and if possible higher resolution data from the input data (Olofsson et al., 2014).

For deforestation detection accuracy:

- *Spatial accuracy*: Application of the Bayesian approach using a high threshold of deforestation probability at which forest changes are confirmed provide high spatial

- accuracy and can be used to detect deforested pixels. Based on this and Reiche et al. (2018) study recommended thresholds are between 0.8 and 0.975.
- *Temporal Accuracy*: Application of the Bayesian approach using a low threshold of deforestation probability at which forest changes are flagged provide high temporal accuracy and can be used to detect deforested dates at previously detected deforested pixels (spatial accuracy). Based on this and (Reiche et al. (2018)) study recommended threshold is 0.5.

References

Achard, F., Stibig, H.-J., Eva, H. D., Lindquist, E. J., Bouvet, A., Arino, O., & Mayaux, P. (2010). Estimating tropical deforestation from Earth observation data. *Carbon Management, 1*(2), 271-287.

Almeida-Filho, R., Shimabukuro, Y., Rosenqvist, A., & Sanchez, G. (2009). Using dual-polarized ALOS PALSAR data for detecting new fronts of deforestation in the Brazilian Amazônia. *International Journal of Remote Sensing, 30*(14), 3735-3743.

Angelsen, A. (2008). REDD models and baselines. *International Forestry Review, 10*(3), 465-475.

Assunção, J., Gandour, C., & Rocha, R. (2014). DETERring deforestation in the Brazilian Amazon: environmental monitoring and law enforcement.

Banskota, A., Kayastha, N., Falkowski, M. J., Wulder, M. A., Froese, R. E., & White, J. C. (2014). Forest monitoring using landsat time series data: A review. *Canadian Journal of Remote Sensing, 40*(5), 362-384.

Boissière, M., Beaudoin, G., Hofstee, C., & Rafanoharana, S. (2014). Participating in REDD+ measurement, reporting, and verification (PMRV): opportunities for local people? *Forests, 5*(8), 1855-1878.

Brofeldt, S., Theilade, I., Burgess, N. D., Danielsen, F., Poulsen, M. K., Adrian, T., . . . Jensen, A. E. (2014). Community monitoring of carbon stocks for REDD+: does accuracy and cost change over time? *Forests, 5*(8), 1834-1854.

Conrad, C. C., & Hilchey, K. G. (2011). A review of citizen science and community-based environmental monitoring: issues and opportunities. *Environmental monitoring and assessment, 176*(1-4), 273-291.

Danielsen, F., Burgess, N. D., Jensen, P. M., & Pirhofer-Walzl, K. (2010). Environmental monitoring: the scale and speed of implementation varies according to the degree of peoples involvement. *Journal of Applied Ecology, 47*(6), 1166-1168.

De Sy, V., Herold, M., Achard, F., Asner, G. P., Held, A., Kellndorfer, J., & Verbesselt, J. (2012). Synergies of multiple remote sensing data sources for REDD+ monitoring. *Current Opinion in Environmental Sustainability, 4*(6), 696-706.

DeVries, B., Pratihast, A. K., Verbesselt, J., Kooistra, L., de Bruin, S., & Herold, M. (2013). *Near real-time tropical forest disturbance monitoring using Landsat time series and local expert monitoring data.* Paper presented at the Analysis of Multi-temporal Remote Sensing Images, MultiTemp 2013: 7th International Workshop on the.

DeVries, B., Pratihast, A. K., Verbesselt, J., Kooistra, L., & Herold, M. (2016). Characterizing Forest Change Using Community-Based Monitoring Data and Landsat Time Series. *PloS one, 11*(3), e0147121.

DeVries, B., Verbesselt, J., Kooistra, L., & Herold, M. (2015). Robust monitoring of small-scale forest disturbances in a tropical montane forest using Landsat time series. *Remote sensing of Environment, 161*, 107-121.

Dutrieux, L. P., Verbesselt, J., Kooistra, L., & Herold, M. (2015). Monitoring forest cover loss using multiple data streams, a case study of a tropical dry forest in Bolivia. *ISPRS Journal of Photogrammetry and Remote Sensing, 107*, 112-125.

Erasmi, S., & Twele, A. (2009). Regional land cover mapping in the humid tropics using combined optical and SAR satellite data—a case study from Central Sulawesi, Indonesia. *International Journal of Remote Sensing, 30*(10), 2465-2478.

European Parliament. (2016). The European Union and forests. Retrieved 10 Nov, 2016, from http://www.europarl.europa.eu/atyourservice/en/displayFtu.html?ftuId=FTU_5.2.11.html

Fagan, M., & DeFries, R. (2009). Measurement and Monitoring of the World's Forests. *Resources for the Future*, 129.

Fry, B. P. (2011). Community forest monitoring in REDD+: the 'M'in MRV? *Environmental Science & Policy, 14*(2), 181-187.

Goodchild, M. F. (2007). Citizens as sensors: the world of volunteered geography. *GeoJournal, 69*(4), 211-221.

Guan, K., Pan, M., Li, H., Wolf, A., Wu, J., Medvigy, D., . . . Malhi, Y. (2015). Photosynthetic seasonality of global tropical forests constrained by hydroclimate. *Nature Geoscience, 8*(4), 284-289.

Gullison, R. E., Frumhoff, P. C., Canadell, J. G., Field, C. B., Nepstad, D. C., Hayhoe, K., . . . Jones, C. D. (2007). Tropical forests and climate policy. *SCIENCE-NEW YORK THEN WASHINGTON-, 316*(5827), 985.

Guyet, T., & Nicolas, H. (2016). Long term analysis of time series of satellite images. *Pattern Recognition Letters, 70*, 17-23.

Haarpaintner, J., Davids, C., Hindberg, H., Zahabu, E., & Malimbwi, R. (2015). Forest and Forest Change Mapping with C-and L-band SAR in Liwale, Tanzania. *The International Archives of Photogrammetry, Remote Sensing and Spatial Information Sciences, 40*(7), 391.

Hamunyela, E., Verbesselt, J., & Herold, M. (2016). Using spatial context to improve early detection of deforestation from Landsat time series. *Remote sensing of Environment, 172*, 126-138.

Hansen, M. C., & Loveland, T. R. (2012). A review of large area monitoring of land cover change using Landsat data. *Remote sensing of Environment, 122*, 66-74.

Hansen, M. C., Potapov, P. V., Moore, R., Hancher, M., Turubanova, S., Tyukavina, A., . . . Loveland, T. (2013). High-resolution global maps of 21st-century forest cover change. *Science, 342*(6160), 850-853.

Harris, N. L., Brown, S., Hagen, S. C., Saatchi, S. S., Petrova, S., Salas, W., . . . Lotsch, A. (2012). Baseline map of carbon emissions from deforestation in tropical regions. *Science, 336*(6088), 1573-1576.

Herold, M. (2009). An assessment of national forest monitoring capabilities in tropical non-Annex I countries: Recommendations for capacity building.

Huang, C., Goward, S. N., Masek, J. G., Thomas, N., Zhu, Z., & Vogelmann, J. E. (2010). An automated approach for reconstructing recent forest disturbance history using dense Landsat time series stacks. *Remote sensing of Environment, 114*(1), 183-198.

Hussain, M., Chen, D., Cheng, A., Wei, H., & Stanley, D. (2013). Change detection from remotely sensed images: From pixel-based to object-based approaches. *ISPRS Journal of Photogrammetry and Remote Sensing, 80*, 91-106.

Kellndorfer, J., Cartus, O., Bishop, J., Walker, W., & Holecz, F. (2014). Large scale mapping of forests and land cover with synthetic aperture radar data. *Land Applications of Radar Remote Sensing*.

Kennedy, R. E., Yang, Z., & Cohen, W. B. (2010). Detecting trends in forest disturbance and recovery using yearly Landsat time series: 1. LandTrendr—Temporal segmentation algorithms. *Remote sensing of Environment, 114*(12), 2897-2910.

Kuplich, T. M. (2006). Classifying regenerating forest stages in Amazonia using remotely sensed images and a neural network. *Forest Ecology and Management, 234*(1), 1-9.

Laurin, G. V., Liesenberg, V., Chen, Q., Guerriero, L., Del Frate, F., Bartolini, A., . . . Valentini, R. (2013). Optical and SAR sensor synergies for forest and land cover mapping in a tropical site in West Africa. *International Journal of Applied Earth Observation and Geoinformation, 21*, 7-16.

Lehmann, E. A., Caccetta, P., Lowell, K., Mitchell, A., Zhou, Z.-S., Held, A., . . . Tapley, I. (2015). SAR and optical remote sensing: Assessment of complementarity and interoperability in the context of a large-scale operational forest monitoring system. *Remote sensing of Environment, 156*, 335-348.

Lehmann, E. A., Caccetta, P. A., Zhou, Z.-S., McNeill, S. J., Wu, X., & Mitchell, A. L. (2012). Joint processing of Landsat and ALOS-PALSAR data for forest mapping and monitoring. *IEEE Transactions on Geoscience and Remote Sensing, 50*(1), 55-67.

Lu, D., Li, G., & Moran, E. (2014). Current situation and needs of change detection techniques. *International Journal of Image and Data Fusion, 5*(1), 13-38.

Lynch, J., Maslin, M., Balzter, H., & Sweeting, M. (2013). Sustainability: Choose satellites to monitor deforestation. *Nature, 496*(7445), 293-294.

Motohka, T., Shimada, M., Uryu, Y., & Setiabudi, B. (2014). Using time series PALSAR gamma nought mosaics for automatic detection of tropical deforestation: A test study in Riau, Indonesia. *Remote sensing of Environment, 155*, 79-88.

Notarnicola, C., Asam, S., Jacob, A., Marin, C., Rossi, M., & Stendardi, L. (2017). *Mountain crop monitoring with multitemporal Sentinel-1 and Sentinel-2 imagery.* Paper presented at the Analysis of Multitemporal Remote Sensing Images (MultiTemp), 2017 9th International Workshop on the.

Olofsson, P., Foody, G. M., Herold, M., Stehman, S. V., Woodcock, C. E., & Wulder, M. A. (2014). Good practices for estimating area and assessing accuracy of land change. *Remote sensing of Environment, 148*, 42-57.

Pratihast, A. K., DeVries, B., Avitabile, V., de Bruin, S., Herold, M., & Bergsma, A. (2016). Design and Implementation of an Interactive Web-Based Near Real-Time Forest Monitoring System. *PloS one, 11*(3), e0150935.

Pratihast, A. K., DeVries, B., Avitabile, V., de Bruin, S., Kooistra, L., Tekle, M., & Herold, M. (2014). Combining satellite data and community-based observations for forest monitoring. *Forests, 5*(10), 2464-2489.

Pratihast, A. K., Herold, M., Avitabile, V., de Bruin, S., Bartholomeus, H., & Ribbe, L. (2012). Mobile devices for community-based REDD+ monitoring: A case study for central vietnam. *Sensors, 13*(1), 21-38.

Rahman, M. M., & Sumantyo, J. T. S. (2010). Mapping tropical forest cover and deforestation using synthetic aperture radar (SAR) images. *Applied Geomatics, 2*(3), 113-121.

Rahman, M. M., & Tetuko Sri Sumantyo, J. (2012). Quantifying deforestation in the Brazilian Amazon using Advanced Land Observing Satellite Phased Array L-band Synthetic Aperture Radar (ALOS PALSAR) and Shuttle Imaging Radar (SIR)-C data. *Geocarto International, 27*(6), 463-478.

Reiche, J. (2015). *Combining SAR and optical satellite image time series for tropical forest monitoring.* Wageningen University.

Reiche, J., de Bruin, S., Hoekman, D., Verbesselt, J., & Herold, M. (2015). A Bayesian approach to combine landsat and ALOS PALSAR time series for near real-time deforestation detection. *Remote Sensing, 7*(5), 4973-4996.

Reiche, J., Hamunyela, E., Verbesselt, J., Hoekman, D., & Herold, M. (2018). Improving near-real time deforestation monitoring in tropical dry forests by combining dense Sentinel-1 time series with Landsat and ALOS-2 PALSAR-2. *Remote sensing of Environment, 204*, 147-161.

Reiche, J., Lucas, R., Mitchell, A. L., Verbesselt, J., Hoekman, D. H., Haarpaintner, J., . . . Woodcock, C. E. (2016). Combining satellite data for better tropical forest monitoring. *Nature Climate Change, 6*(2), 120-122.

Riechmann, D. (2007). Literature Survey on biological data and research carried out in Bonga area, Kafa, Ethiopia. *PPP-Project Introduction of sustainable coffee production and marketing complying with international quality standards using the natural resources of Ethiopia. Ethiopia, NABU*.

Rosenqvist, A., Shimada, M., Ito, N., & Watanabe, M. (2007). ALOS PALSAR: A pathfinder mission for global-scale monitoring of the environment. *IEEE Transactions on Geoscience and Remote Sensing, 45*(11), 3307-3316.

Ryan, C. M., Hill, T., Woollen, E., Ghee, C., Mitchard, E., Cassells, G., . . . Williams, M. (2012). Quantifying small-scale deforestation and forest degradation in African woodlands using radar imagery. *Global Change Biology, 18*(1), 243-257.

Schmitt, C. B., Denich, M., Demissew, S., Friis, I., & Boehmer, H. J. (2010). Floristic diversity in fragmented Afromontane rainforests: Altitudinal variation and conservation importance. *Applied Vegetation Science, 13*(3), 291-304.

Schmitt, C. B., Senbeta, F., Denich, M., Preisinger, H., & Boehmer, H. J. (2010). Wild coffee management and plant diversity in the montane rainforest of southwestern Ethiopia. *African Journal of Ecology, 48*(1), 78-86.

Shimada, M. (2010). Ortho-rectification and slope correction of SAR data using DEM and its accuracy evaluation. *IEEE Journal of Selected Topics in Applied Earth Observations and Remote Sensing, 3*(4), 657-671.

Shimada, M., Itoh, T., Motooka, T., Watanabe, M., Shiraishi, T., Thapa, R., & Lucas, R. (2014). New global forest/non-forest maps from ALOS PALSAR data (2007–2010). *Remote sensing of Environment, 155*, 13-31.

Skarlatidou, A., Haklay, M., & Cheng, T. (2011). Trust in Web GIS: the role of the trustee attributes in the design of trustworthy Web GIS applications. *International Journal of Geographical Information Science, 25*(12), 1913-1930.

Skutsch, M. M., Torres, A. B., Mwampamba, T. H., Ghilardi, A., & Herold, M. (2011). Dealing with locally-driven degradation: A quick start option under REDD+. *Carbon balance and management, 6*(1), 1-7.

Strahler, A. H. (1980). The use of prior probabilities in maximum likelihood classification of remotely sensed data. *Remote sensing of Environment, 10*(2), 135-163.

UNFCCC. (2009). Methodological guidance for activities relating to reducing emissions from deforestation and forest degradation and the role of conservation, sustainable management of forests and enhancement of forest carbon stocks in developing countries. Decision 4/CP. 15. See h ttp. *unfccc. int/resource/docs/2009/cop15/eng/11a01. pdf# page, 11*.

Verbesselt, J., Zeileis, A., & Herold, M. (2012). Near real-time disturbance detection using satellite image time series. *Remote sensing of Environment, 123*, 98-108.

Walker, W. S., Stickler, C. M., Kellndorfer, J. M., Kirsch, K. M., & Nepstad, D. C. (2010). Large-area classification and mapping of forest and land cover in the Brazilian Amazon: a comparative analysis of ALOS/PALSAR and Landsat data sources. *IEEE Journal of Selected Topics in Applied Earth Observations and Remote Sensing, 3*(4), 594-604.

Wheeler, D., Hammer, D., Kraft, R., & Steele, A. (2014). Satellite-based forest clearing detection in the Brazilian Amazon: FORMA, DETER, and PRODES. *World Resources Institute: Washington, DC, USA*.

Whittle, M., Quegan, S., Uryu, Y., Stüewe, M., & Yulianto, K. (2012). Detection of tropical deforestation using ALOS-PALSAR: A Sumatran case study. *Remote sensing of Environment, 124*, 83-98.

Zarin, D. J. (2012). Carbon from tropical deforestation. *Science, 336*(6088), 1518-1519.

Zhang, J. (2010). Multi-source remote sensing data fusion: status and trends. *International Journal of Image and Data Fusion, 1*(1), 5-24.

Zhu, Z., Woodcock, C. E., & Olofsson, P. (2012). Continuous monitoring of forest disturbance using all available Landsat imagery. *Remote sensing of Environment, 122*, 75-91.